Journal of proteome research

Cite This: J. Proteome Res. XXXX, XXX, XXX−XXX

Article

pubs.acs.org/jpr

Proteome Comparisons between Hemolymph of Two Honeybee Strains (*Apis mellifera ligustica*) Reveal Divergent Molecular Basis in Driving Hemolymph Function and High Royal Jelly Secretion

Zewdu Ararso,[†] Chuan Ma,[†] Yuping Qi, Mao Feng, Bin Han, Han Hu, Lifeng Meng, and Jianke Li*

Institute of Apicultural Research/Key Laboratory of Pollinating Insect Biology, Ministry of Agriculture, Chinese Academy of Agricultural Sciences, Beijing 100081, China

Supporting Information

ABSTRACT: Hemolymph is vital for the immunity of honeybees and offers a way to investigate their physiological status. To gain novel insight into the functionality and molecular details of the hemolymph in driving increased Royal Jelly (RJ) production, we characterized and compared hemolymph proteomes across the larval and adult ages of Italian bees (ITbs) and Royal Jelly bees (RJbs), a stock selected from ITbs for increasing RJ output. Unprecedented in-depth proteome was attained with the identification of 3394 hemolymph proteins in both bee lines. The changes in proteome support the general function of hemolymph to drive development and immunity across different ages. However, age-specific proteome settings have adapted to prime the distinct physiology for larvae and adult bees. In larvae, the proteome is thought to drive temporal immunity, rapid organogenesis, and reorganization of larval structures. In adults, the proteome plays key roles in prompting tissue development and immune defense in newly emerged bees, in gland maturity in nurse bees, and in carbohydrate energy production in forager bees. Between larval and adult samples of the same age, RJbs and ITbs have tailored distinct hemolymph proteome programs to drive their physiology. In particular, in day 4 larvae and nurse bees, a large number of highly abundant proteins are enriched in protein synthesis and energy metabolism in RJbs. This implies that they have adapted their proteome to initiate different developmental trajectories and high RJ secretion in response to selection for enhanced RJ production. Our hitherto unexplored in-depth proteome coverage provides novel insight into molecular details that drive hemolymph function and high RJ production by RJbs.

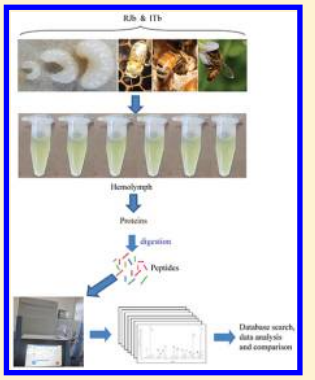

KEYWORDS: *proteome, hemolymph, Royal Jelly bees, Italian bees*

1. INTRODUCTION

Hemolymph of insects circulates throughout the body cavity (hemocoel) serving several biological functions, such as transportation of biological molecules, nutrients, and hormones.[1,2] Although the principal function of hemolymph is to transport materials through the insects' body, the immune agent it contains is vital for the formation of the primary line of defense against invading microorganisms.[3,4] This is due to the presence of an innate immune system consisting of humoral defense, the production of reactive molecules, and cellular defense, phagocyte-mediated phagocytosis and encapsulation.[5,6] Given its biological functions, hemolymph is suitable for evaluating systemic changes in the insect's body.[3,7]

As in other insects, hemolymph of honeybees is composed of wide ranges of organic and inorganic substances, such as microphage-like cells, salts, proteins, lipids, carbohydrates, nucleic acids, hormones, as well as degradation products of these compositions.[1,3,4,8] Variations in hemolymph proteins can be used to investigate phenotypical and physiological differences among honeybees.[2,9−11] These variations have been reported in several hemolymph proteomic studies. For instance, the difference in hemolymph proteome between red-eye pupae and newly emerged bees (NEBs) indicates the occurrence of protein depletion due to metabolic use during body reconstruction of the red-eye pupae.[11,12] Innate immunity is positively correlated with age development of larvae.[13] Moreover, it is suggested that high abundance levels of ferritin, glutamine S-transferase, and toll-like receptor 13 in the hemolymph of NEBs function as an adaptation in the innate immune system to the new environment upon emerging.[11] Furthermore, adult honeybee workers express strong humoral immune reactions in their hemolymph upon artificial bacterial challenge.[6] In immunized adult drones, genes related to peptidoglycan recognition protein-S2 and lysosome 2 are distinctively up-regulated.[14]

China has now genetically bred a honeybee line to increase RJ production for over four decades from ITbs, *Apis mellifera ligustica*, RJbs. A colony of RJbs can produce 10 kg of RJ a year, which is at least 10 times more than the RJ production of ITbs.[15] About 4000 tons of RJ is produced annually, accounting for >90% of the world's total output.[16] The increased RJ production by RJbs is related to genetic dominant traits for high RJ production[17−19] and larger arcini size of hypophar-

Received: September 1, 2017
Published: November 27, 2017

DOI: 10.1021/acs.jproteome.7b00621
J. Proteome Res. XXXX, XXX, XXX−XXX

yngeal glands (HGs), where RJ is secreted.[20] Compared with ITbs, the HGs of winter RJb workers store more nitrogen-containing brood food to physiologically prepare for the upcoming brood rearing during the spring colony buildup.[21] Three-day old workers of RJbs have potentially activated the gland activity for secretion of RJ, earlier than the activation in ITbs.[22] Moreover, RJbs have shown altered proteome settings to drive the enlarged HGs and enhanced gland performance through stronger expression of proteins associated with cytoskeleton and protein biosynthesis, which, in turn, consolidates the secretion of voluminous RJ.[20] Furthermore, neural peptides regulating behaviors of RJ secretion in RJbs are enhanced in the brain via regulation of water homeostasis, brood pheromone recognition, foraging capacity, and pollen collection to underline the elevated physiology of RJ secretion.[23] These observations demonstrate the fact that genetic selection for increased RJ outputs has reshaped the proteome and neuropeptidome signatures in RJbs to fit to the physiology required for higher RJ output. We expect that the aforementioned changes in physiology and proteome to support the high RJ yield in RJbs should be reflected in alterations in the hemolymph proteome.

The rapid technological development of mass spectrometer (MS) in resolution, sensitivity, and mass accuracy has made it possible to identify thousands of proteins in a single sample. MS-based proteomics has become widely employed in honeybee science to uncover a wide spectrum of biological issues, such as embryogenesis,[24,25] HG and brain functions,[26,27] larval development,[13] resistance to *Varroa* and sack brood diseases,[28,29] and the hemolymph itself.[9,11,10] Despite several proteomic studies to dissect the molecular underpinnings of the hemolymph functions, only a limited proteome coverage could be achieved in honeybees. For instance, only 324 proteins were identified by applying MS-based proteomics in hemolymph of queens, drones, workers, and worker larvae, revealing profound proteome differences among the castes,[2] and 129 proteins were identified in the hemolymph of red-eyed pupae of worker bees by two-dimensional electrophoresis (2-DE)-based proteomics. Many of these proteins were involved in the mechanism of metamorphosis as well.[12] This is mainly due to the technical limitations of low sensitivity and resolution of MS from about a decade ago, in which merely a small fraction of proteins is identified. In recent times, over 2000 proteins can be identified in the hemolymph of the honeybee pupae with the application of state-of-the-art MS-based proteomics. This extended proteome coverage helped us gain new insight into the key roles of hemolymph proteins in the immune response of *Varroa* sensitive hygienic bees to fight against mite infestation.[29] However, these studies have a relatively low proteome coverage (around 2000 proteins), which covers only a limited part of the developmental process. Hence, a deep proteome profiling is encouraged to enhance the understanding of the molecular underpinnings of hemolymph. Moreover, it is unknown how hemolymph proteome underlines the enhanced RJ yields of RJbs, as compared with that in ITbs, which remains lacking. Therefore, the aim of this work is to characterize the hemolymph proteome in-depth in RJbs and ITbs and compare the proteome differences between both stocks to gain novel insight into the functionality of hemolymph and the molecular details of hemolymph in driving increased RJ production of RJbs.

2. MATERIALS AND METHODS

2.1. Chemical Reagents

LC−MS-grade methanol (cat. no. A456-4), acetonitrile (cat. no. A955-4), and water (cat. no. W6-4) were obtained from Fisher Scientific. HPLC-grade formic acid (cat. no. 50144) was obtained from Dikma. Modified sequencing-grade trypsin (cat. no. V5111) was obtained from Promega (Madison, WI).

2.2. Hemolymph Sampling

Artificially mated RJb and ITb queens were purchased from Pinghu honeybee breeding station, Zhejiang Province, China and Bologna, Italy, respectively, and kept for colony build-up in the apiary of the Institute of Apicultural Research, Chinese Academy of Agricultural Sciences in Beijing. Five colonies of each bee strain with similar colony strength were selected as the experimental colonies. For larval hemolymph collection, each queen was caged in a single comb frame containing worker cells for 6 h in each colony to collect larvae of known ages. Then, the queens were unconfined from the cages and the eggs contained in the cells of the frames were kept in their respective colonies for further development. Hemolymph samples were collected from the larvae on day 2 (d2), day 4 (d4), and day 6 (d6), following our previously published protocol.[9] Before hemolymph collection, all larvae were washed twice with phosphate-buffered saline (PBS) to eliminate possible contamination with RJ during feeding by nurse bees (NBs) in the comb cells. For d2 larvae, hemolymph was collected by piercing their skins with great care to evade damaging their organs. For d4 and d6 larvae, hemolymph was collected by inserting a disposable glass microcapillary pipet (5 μL) into one side (two-thirds down from head) of the larva, avoiding deep cuts and sucking the hemolymph by capillary action. For adult stages, the NEBs that emerged from comb cells <10 h were marked on their thoraxes and placed back into colonies for subsequent development, while others were directly sampled. The marked NEBs were collected on day 10 as samples of NBs. Forager bees (FBs) with pollen loads were collected at the entrances of hives (~20 days old). After obtaining bee samples, the bees were anesthetized using CO_2. Hemolymph was collected from the dorsal vessel using a glass capillary tube (40 μm outer diameter) by piercing the intersegmental membrane between the fourth and fifth tergites of the adult abdomen, as described elsewhere.[8] For each strain at each time point, 100 μL of hemolymph was collected from five colonies. Three independent biological replicates per time point were prepared. All of the collected hemolymph samples were stored at −80 °C until used.

2.3. Royal Jelly Collection

To compare RJ production between RJbs and ITbs, the same five colonies of each honeybee stock were used as for hemolymph sampling described above. Each colony was provided with 132 plastic queen cell cups with larvae grafted in per replication. RJ collections were performed approximately after 60−70 h. RJ collection of three batches from each strain was done and weighed with a digital scale. RJ yield difference between the two stocks was compared using the Student's *t*-test ($p < 0.05$).

2.4. Protein Preparation and Digestion

Protein extraction was done following a method previously described.[26] In brief, hemolymph homogenates were mixed with a lysis buffer (8 M urea, 2 M thiourea, 4% CHAPS, 20 mM Tris-base, 30 mM dithiothreitol (DTT), 2% Biolyte (pH 3−10)), and protease inhibitor (Roche, Basel, Switzerland) on ice

DOI: 10.1021/acs.jproteome.7b00621
J. Proteome Res. XXXX, XXX, XXX−XXX

for 30 min and then centrifuged at 15 000g at 4 °C for 20 min. Three volumes of ice-cold acetone were added to the recovered supernatant and kept for 30 min for protein precipitation and desalting, followed by centrifuging at 15 000g at 4 °C for 20 min. The precipitated protein was resuspended in 100 μL of 5 M urea and then dissolved in 4 volumes of 40 mM NH_4HCO_3. Protein concentration was determined using a Bradford assay based on our published protocols.[29,30] Protein samples were mixed with 10 mM DTT solution for 1 h to prevent reformation of disulfide bonds and finally incubated in 50 mM iodoacetamide for alkylation at room temperature for 1 h under the dark condition. Proteins were digested using sequencing-grade trypsin in a volume ratio of 1:50 (enzyme to protein) at 37 °C overnight, and 1 μL of formic acid was added to the solution to stop the enzymatic digestion. Then, peptides were dried using a SpeedVac system (RVC 2−18, Marin Christ, Osterod, Germany) for the subsequent LC−MS/MS analysis.

2.5. LC−MS/MS Analysis

The dried peptides were dissolved in 0.1% formic acid and loaded onto a LC−MS system with three replications of each sample. Peptides were separated by nanoflow liquid chromatography on an EASY-nLC 1000 system (Thermo Fisher Scientific) coupled to a Q Exactive mass spectrometer (Thermo Fisher Scientific). Peptide enrichment was done with a trap column (5.0 μm Aqua C18 beads, 2 cm long, 100 μL inner diameter fused silica, Thermo Fisher Scientific). Separation was achieved with an analytical column (15 cm long, 75 μm inner diameter fused silica column filing with 3.0 μm Aqua C18 beads, Thermo Fisher Scientific). Peptides were separated chromatographically by using a 120 min gradient from 8 to 30% acetonitrile in 0.1% formic acid with a flow rate of 350 nL/min. Spray voltage was set between 2.4 and 2.6 kV. The instrument was operated in a data-dependent mode. The following settings were applied: one full scan resolution at 70 000, scan range: m/z 300−1800; followed by top 20 MS/MS scans using high-energy collision-induced dissociation mode at a resolution of 17 500, isolation window 2 m/z, normalized collision energy of 27, and loop count 20 using dynamic exclusion (charge exclusion: unassigned 1, 8, >8; peptide match: preferred; exclude isotopes: on; dynamic exclusion: 10 s). The MS/MS spectra were retrieved using Xcalibur software (version 2.2, Thermo Fisher Scientific) and saved as raw files. Each sample was run with technical injections in three replicates. The LC−MS/MS data have been deposited to the ProteomeXchange Consortium (http://proteomecentral.proteomexchange.org) via the PRIDE partner repository with the data set identifier PXD007824.

2.6. Protein Identification and Quantification of Abundance

For protein identification, PEAKS software (version 7.5, Bioinformatics Solutions) was used by searching the raw MS files against the database of protein sequences of *Apis mellifera* downloaded from NCBI (Feb 2015) and the common contaminant, with a total of 21 778 entries. The search criteria were: specificity: trypsin; fixed modification: carbamidomethyl; and oxidation as a variable modification, with two allowed missed cleavages per peptide; three maximum allowed variable PTM per peptide. Precursor and fragment mass tolerances were 20.0 ppm and 0.05 Da, respectively. False discovery rate (FDR) was controlled by using a fusion strategy of target and decoy database for both protein and peptide level identifications applying a threshold of ≤1.0%, an enhanced target-decoy approach that makes more conservative FDR estimations.[31] A protein was only considered an identified protein when at least one unique peptide with at least two spectra was identified.

To quantify the level change of protein abundance across the six time points of larvae and adult in each bee stock and at each time point between the stocks, label-free approach quantitation module of the PEAKS software was used. Feature detection was carried out on each sample using the expectation-maximization algorithm, and a high-performance retention time alignment algorithm was used to align the features of the same peptide, from three replicates of each sample, to an automatically selected reference by the PEAKS software.[32] Normalization was done by a factor of the samples by dividing the total ion current (TIC) multiple by the TIC of the reference sample. To obtain the abundance levels of proteins, the top three abundant peaks intensity of the tryptic peptides of a protein were summed. The alteration levels of protein abundance were compared across six time points in each bee line and at six time points between the two stocks. The abundance differences of a protein between different samples were considered statistically significant when both p value <0.05 and fold change ≥1.5 were attained. Hierarchical clustering was performed to cluster expressional profile of differentially abundant protein using uncentered Pearson correlation and average linkage in PEAKS software.

2.7. Bioinformatics Analysis

The biological categories and KEGG pathways were enriched using ClueGO v2.1.7, a Cytoscape plug-in (http://www.ici.upmc.fr/cluego),[33] to assign the identified proteins into specific gene ontology (GO) terms. The significantly enriched functional GO categories and pathways were tested using a right-sided hypergeometric test comparing proteins identified from the samples to the background set of GO annotations in the entire *Apis mellifera* genome. The FDR was controlled by the Bonferroni step-down test to correct the p value, and the GO terms were considered to be significantly enriched when the corrected p value was <0.05.

To gain further insight into the possible functional linkages among the highly abundant proteins of each stage, protein−protein interaction (PPI) networks were constructed by GeneMANIA, a Cytoscape plug-in.[34] The known and predicted PPI data sets from *Drosophila melanogaster* were searched in GeneMANIA with the following parameters: all networks enabled, equal weighting by GO biological process, and the top 20 genes displayed. The GO category enrichment of the input data set was compared with the background set of GO annotations in the whole *Drosophila melanogaster* genome using a right-sided hypergeometric test. FDR was controlled by q value. Proteins were grouped according to their GO annotations, and the networks were visualized in Cytoscape.

2.8. Metabolomics Analysis

To test the most divergent ages (d4 larvae and NBs) in proteome data between RJbs and ITbs, hemolymph samples (n = 6) of d4 larvae and NBs were prepared from both bee stocks, as described above for the proteomic analysis. To precipitate protein and extract metabolites, 30 μL of hemolymph was added to 120 μL of cold methanol, and N-formylanthranilic acid was added as an internal standard (36 ng/μL). The mixture was vortexed for 30 s, ultrasonicated for 30 min, and kept at −20 °C for 20 min. After centrifugation at 16 000g for 20 min at 4 °C, 90 μL of the supernatant was collected for LC−MS analysis.

DOI: 10.1021/acs.jproteome.7b00621
J. Proteome Res. XXXX, XXX, XXX−XXX

A UHPLC system (Dionex Ultimate 3000, Thermo Fisher Scientific) was coupled to a Q Exactive mass spectrometer (Thermo Fisher Scientific) with a Heated Electrospray Ionization Source I (HESI). The separation of compounds was performed on a ZORBAX SB-Aq C18 reversed-phase column (100 mm × 2.1 mm, 1.8 μm; Agilent Technology, USA) at 50 °C. A gradient elution program was run for chromatographic separation with mobile phase A (water with 0.1% formic acid) and B (acetonitrile with 0.1% formic acid) as follows: 0−1 min, 95−95% A; 1−10 min, 95−0% A; 10−16 min, 0−0% A; and 16−18 min, 0−95% A; and 18−25 min, 95−95% A. Samples of 3 μL were injected with a flow rate of 0.2 mL/min. Sample analyses were separately performed in positive (ESI+) and negative ion (ESI−) modes. At the beginning of the LC−MS run, six injections of a quality-control (QC) sample, which was prepared by pooling equal volumes of hemolymph from each of the 24 samples and extracting metabolites, were applied to condition the column. The QC sample was then injected once before every six real samples and once again at the end of the run. These QC injections (a total of 5) were to measure the stability and performance of the system and to calculate RSD of each feature. All 24 samples were injected in a randomized order to avoid systematic errors.

The HESI parameters were optimized as follows: sheath gas flow rate 40; aux. gas flow rate 5; spray voltage 3500 V for ESI+ and 3000 V for ESI−; capillary temperature 320 °C; S lens RF level 60; and aux. gas heater temperature 350 °C. Full scan data (m/z 80−1000) in both ESI+ and ESI− modes were acquired at a resolution of 70 000. The automatic gain control (AGC) was set at 1×10^6 and the maximum injection time was set to 50 ms. Scan rate was set at 1 scan/s.

For compound identification, MS detection was performed with alternation between full MS and data-dependent MS^2 scan (dd-MS^2). The full MS settings were as described above, whereas the dd-MS^2 settings were as follows: scan resolutions 17 500; AGC target 1×10^5; maximum injection time 50 ms; loop count 10; isolation window 4.0 m/z; and stepped (N)CE 10, 25, and 40.

The raw MS data were converted into the ".mzXML" format using Proteowizard[35] and were processed with the XCMS package[36] using the R platform for the baseline filter, peak identification and calculation, and retention time alignment. The XCMS centWave method was used to identify the peaks: ppm parameter, 5; peak width, 5−20 s; and signal/noise threshold, 4. The obiwarp method was used to align the retention time. Finally, a 2D matrix of data, mass-charge ratio (m/z) and retention time for each feature, was obtained. Only features with a peak area above 1×10^7 for five or six biological replicates of at least one sample group were used for further analysis. The peak area of each feature was normalized to that of the internal standard (*N*-formylanthranilic acid). Moreover, features with poor repeatability, that is, features with RSD values >20% for the five QC injections, were removed from subsequent analysis as suggested elsewhere.[37]

To detect classification of the samples, Principal Component Analysis (PCA) and Hierarchical Cluster Analysis (HCA) were performed in SIMCA 13.0 (Umetrics, Umea, Sweden) with Pareto scaling. To maximize identification of differences in metabolic profiles between groups, an orthogonal projection to latent structure-discriminant analysis (OPLS-DA) model was applied using SIMCA 13.0 with Pareto scaling. The Variable Importance for the Projection (VIP) of each feature was calculated to indicate its contribution to the classification. A Student's *t*-test was used to assess the statistical difference between the hemolymph of two bee stocks. Features with p values <0.05 and VIP values >1 were considered to be differential features between the hemolymph of two bee stocks.

Accurate masses of differential features were searched against online databases including the METLIN (http://metlin.scripps.edu), HMDB (http://hmdb.ca), and LIPID MAPS (http://lipidmaps.org) with mass tolerance of 10 ppm. The identity of compounds was confirmed by searching feature fragments from LC−MS/MS against METLIN, HMDB, LIPID MAPS, and MetFrag (https://msbi.ipb-halle.de/MetFrag/). The compound identity was accepted if the masses of a feature and at least two of its fragments matched those (m/z < 10 ppm) in one of these database. The identified compounds were imported into MBROLE 2.0[38] with *A. mellifera* as the background set to conduct KEGG pathway analysis. The p values were adjusted by controlling the false discovery rate (FDR).[39] Pathways with FDR values of <0.05 were regarded as significantly enriched metabolic pathways.

2.9. Western Blotting Analysis

To confirm abundance level changes in proteins between d4 larvae of RJbs and ITbs; and NBs of each stock, Western Blotting analysis was performed. Primary rabbit polyclonal antibodies (Genecreat, Wuhan, China), anti-RpS6 (unique to RJbs) for d4 larvae samples and *anti*-adenylate kinase (50-fold in RJbs) for NBs samples, at dilutions of 1:3000 were used. A secondary antibody (Genecreat, Wuhan, China), horseradish peroxidase-conjugated goat antirabbit, at a dilution of 1:5000 was used. Samples of ∼10 μg of protein were sequentially separated by stacking (4%) and separating (12%) SDS-PAGE gels, and each sample was run in triplicate. The protein samples were transferred to nitrocellulose membranes (0.2 μm pore size, Invitrogen, Eugene, OR) with an iBlot apparatus (Invitrogen, CA). The bands of protein were visualized by chemiluminescence and quantified by densitometry using Quantity-one image analysis software (Bio-Rad, Hercules, CA). The protein abundance was normalized by GAPDH and analyses by Student's *t*-tests.

3. RESULTS

3.1. Comparison of Royal Jelly Production

To compare RJ production between RJbs and ITbs, RJ yields of five colonies of each stock were analyzed. RJbs produced significantly (p < 0.001) higher amounts of RJ (99.15 ± 3.57 g) as compared with ITbs (7.20 ± 2.63 g) (Figure 1).

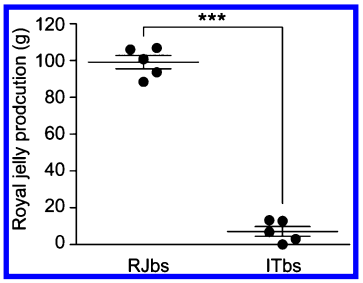

Figure 1. RJ production comparison between RJbs and ITbs. The data are shown as mean ± SE ***, p < 0.001; n = 5.

DOI: 10.1021/acs.jproteome.7b00621
J. Proteome Res. XXXX, XXX, XXX−XXX

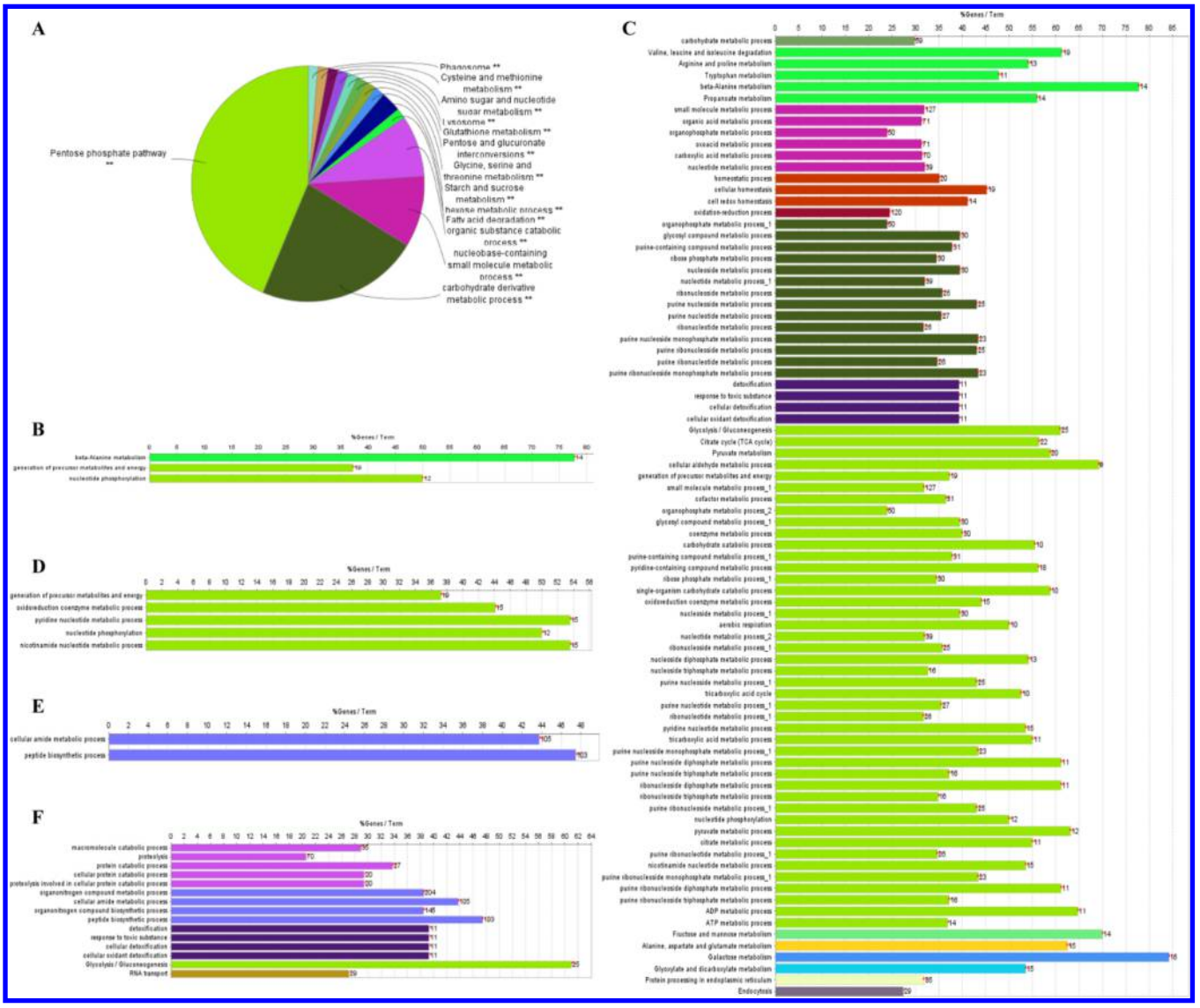

Figure 2. Qualitative comparison of identified hemolymph proteins across six time points of RJbs. The identified proteins in the hemolymph of RJbs over six time points were analyzed using ClueGO to compare the functional classes and pathways specifically enriched by proteins at each time points. Pie chart (A) shows the significantly enriched functional classes and pathways shared among six time points. Bar charts B, C, D, E, and F indicate specifically enriched functional classes and pathways in day 2, 4, and 6 larvae, NEBs, and NBs, respectively. Note: Name of each functional class or pathway is assigned by the lowest p value of the terms of the class. The same color is indicates that the terms are categorized under the same functional group. The single and double asterisks indicate significant enrichment at $p < 0.05$ and $p < 0.01$statistical levels, respectively.

3.2. Hemolymph Proteome Comparison of RJbs across Six Time Points of Larval and Adult Stages

To understand the biological importance of the proteome that underlines the transition from larva to adult, hemolymph proteomes were compared across six time points in RJbs. 739, 1322, 813, 1380, 1457, and 710 proteins were identified in d2, d4, d6 brood, NEBs, NBs, and FBs, respectively, representing 2796 nonredundant proteins (Tables S1−S6). These proteins were enriched in four functional classes and 10 pathways that overlapped across six time points (Figure 2A, Table S7). For example, amino sugar and nucleotide sugar metabolism, organic substance catabolic process, and glutathione metabolism were among the strongly enriched. However, nucleotide phosphorylation and beta-alanine metabolism were exclusively enriched in d2 larvae (Figure 2B, Table S7). In d4 larvae, the following functional classes, small-molecule metabolic process, oxidation−reduction process, and carbohydrate metabolic process, and the following pathways, galactose metabolism, alanine, aspartate and glutamate metabolism, endocytosis, protein processing in endoplasmic reticulum (ER), and glyoxylate and dicarboxylate metabolism, were uniquely enriched (Figure 2C, Table S7). Only pyridine nucleotide metabolic process was enriched in d6 larvae (Figure 2D, Table S17). In adult bees, only peptide biosynthetic process was uniquely enriched in NEBs (Figure 2E, Table S7). Three functional classes, protein catabolic process, organonitrogen compound metabolic process, and response to toxic substance, and one pathway, RNA transport, were distinctively enriched in NBs (Figure 2F, Table S7). However, no unique functional class or pathway was significantly enriched in FBs.

Of the 2796 proteins in RJbs found across six time points, 241 proteins were significantly regulated, of which 12, 53, 9, 70, 60, and 37 proteins were highly abundant in d2, d4, d6 larvae, NEBs, NBs, and FBs, respectively (Figure 3A, Table S8). The

DOI: 10.1021/acs.jproteome.7b00621
J. Proteome Res. XXXX, XXX, XXX−XXX

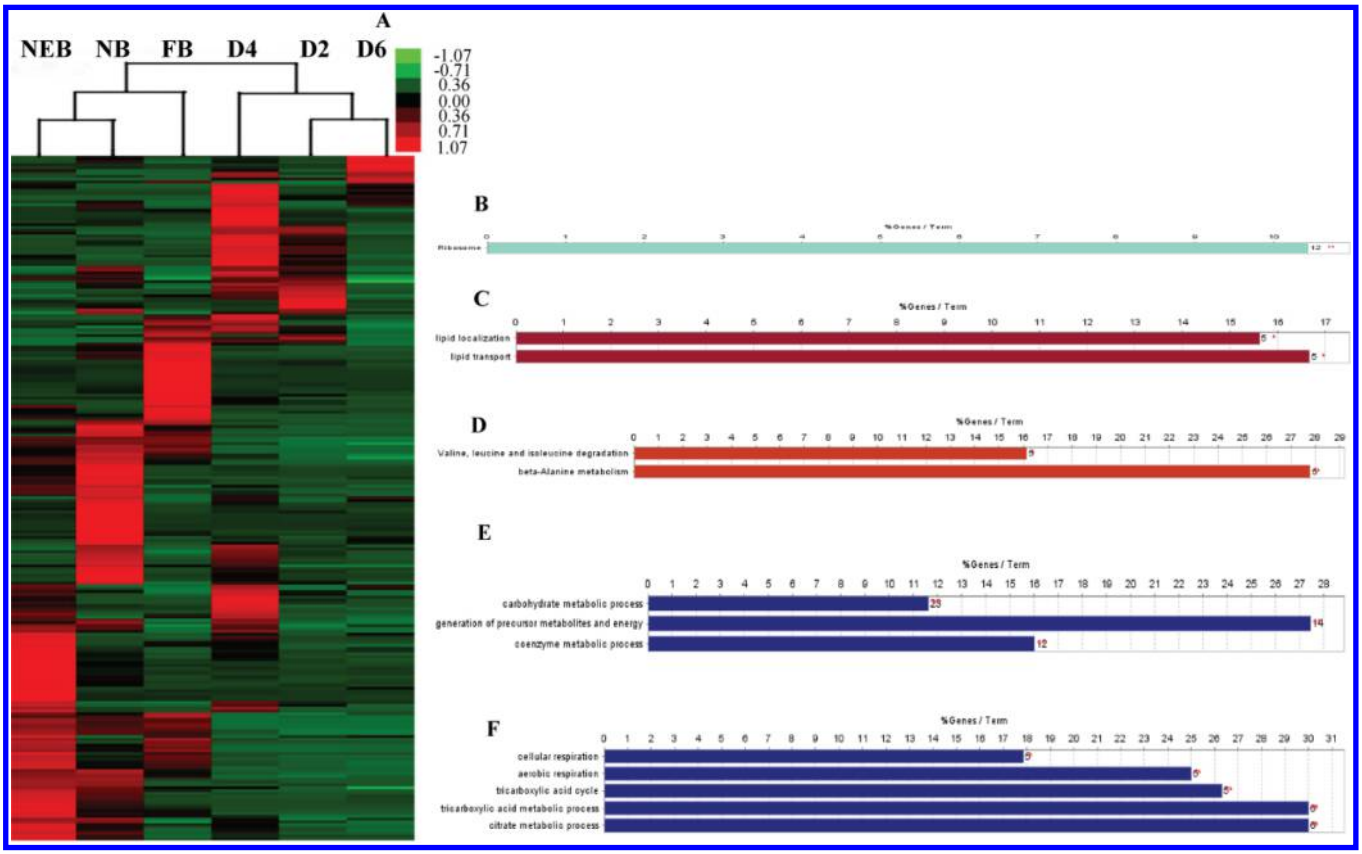

Figure 3. Quantitative comparison of RJb hemolymph proteins over six time points. The unsupervised hierarchical clustering analysis of proteins with altered abundance levels (fold change >1.5 and $p < 0.05$); the columns indicate the time points, and the rows represent individual proteins (A). The up-regulated proteins are indicated by red color and the down-regulated ones by green color. The color intensity changes with the protein expression level as indicated on the key bar. Bar charts B, C, D, E, and F indicate enriched specific terms in day 4 and 6 larvae, NEBs, NBs, and FBs, respectively. The single and double asterisks indicate significant enrichment at $p < 0.05$ and $p < 0.01$ statistical levels, respectively.

12 highly abundant proteins in d2 were not enriched in any functional class or pathway. The 53 highly abundant proteins in d4 larvae were enriched in ribosome pathway (Figure 3B, Table S9). The nine highly abundant proteins in d6 larvae were enriched in lipid transport (Figure 3C, Table 9). Furthermore, the highly abundant proteins in NEBs were only enriched in the pathway of beta-alanine metabolism (Figure 3D, Table S9). Lastly, the highly abundant proteins in NBs and FBs were significantly enriched in the generation of precursor metabolites and energy and citrate metabolic process, respectively (Figure 3E,F, Table S9).

As for the highly abundant proteins linked in a RJbs PPI network, ribosome (q-value = 1.30×10^{-6}), chemical homeostasis (q-value = 1.28×10^{-2}), and translational elongation (q-value = 2.55×10^{-2}) were significantly enriched in d4 larvae (Figure S1A). Likewise, protein folding (q-value = 2.00×10^{-5}), cellular amino acid metabolic process (q-value = 1.69×10^{-3}), and mitochondrial transport (q-value = 3.28×10^{-2}) were significantly enriched in NEBs (Figure S1B). Glycolysis (q-value = 3.62×10^{-4}), generation of precursor metabolites and energy (q-value = 8.94×10^{-4}), and antioxidant activity (q-value = 7.51×10^{-3}), were significantly enriched in NBs (Figure S1C). Tricarboxylic acid cycle (q-value = 5.46×10^{-7}) was enriched in FBs (Figure S1D).

3.3. Hemolymph Proteome Comparison of ITbs across Six Time Points of Larval and Adult Stages

Regarding ITbs, 836, 1057, 820, 1014, 1090, and 759 proteins were identified in the hemolymph of d2, d4, d6 larvae, NEBs, NBs, and FBs, respectively, representing 2469 nonredundant proteins (Tables S10–S15). Six functional classes and 11 pathways were significantly enriched and shared over the six time points. Glycolysis/gluconeogenesis was the strongest enriched pathway, followed by organic substance catabolic process and phagosome (Figure 4A, Table S16). Two pathways, beta-alanine metabolism and lysosome, were uniquely enriched in d2 larvae (Figure 4B, Table S16). Three functional classes, small-molecule metabolic process, carboxylic acid metabolic process, and oxidation–reduction, and two pathways, galactose, and alanine, aspartate, and glutamate metabolisms, were exclusively enriched in d4 larvae (Figure 4C, Table S16). No functional classes or pathways were uniquely enriched in d6 larvae. In NBs, two functional classes, organonitrogen compound metabolic process and regulation of protein metabolic process were exclusively enriched (Figure 4D, Table S16). Only functional class of pyridine-containing compound metabolic process was uniquely enriched in FBs (Table S16).

Among the 2469 proteins identified in ITbs over six time points, the expression levels of 220 proteins were changed. There were 9, 11, 9, 83, 43, and 65 proteins highly abundant in d2, d4, d6 larvae, NEBs, NBs, and FBs, respectively (Figure 5A, Table S17). Unlike in RJbs, the highly abundant proteins in the three larval stages of ITbs were not enriched in any functional class or pathway. However, the 83 highly abundant proteins in NEBs were significantly enriched in three pathways: lysosome, arginine biosynthesis, and protein processing in ER (Figure 5B,

DOI: 10.1021/acs.jproteome.7b00621
J. Proteome Res. XXXX, XXX, XXX–XXX

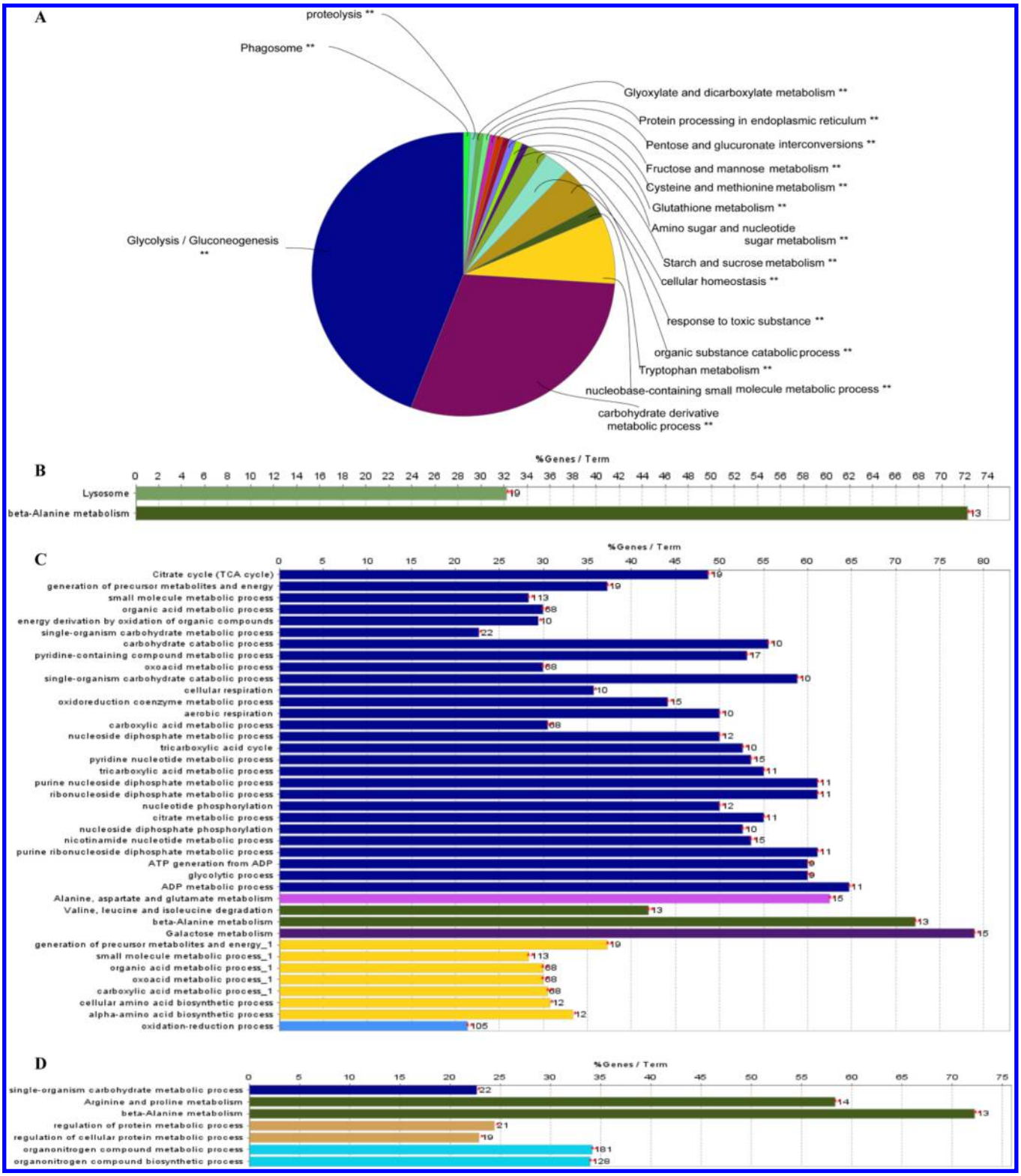

Figure 4. Qualitative comparison of identified hemolymph proteins over six time points of ITbs. The identified proteins in the hemolymph of ITbs over six time points were analyzed using ClueGO to compare the functional classes and pathways specifically enriched by proteins at each time points. Pie chart (A) displays the significantly enriched functional classes and pathways shared among six time points. Bar charts B, C, and D indicate specifically enriched functional classes and pathways in d2 and d4 larvae, and NBs, respectively. The single and double asterisks indicate significant enrichment at the $p < 0.05$ and $p < 0.01$ statistical levels, respectively.

Table S18). The 43 highly abundant proteins in NBs were significantly enriched in single-organism carbohydrate metabolic process and pentose and glucuronate interconversions (Figure 5C, Table S18). The 65 highly abundant proteins in FBs were enriched in the functional classes and pathway: response to toxic substance, chemical homeostasis, cellular carbohydrate metabolic process, and galactose metabolism (Figure 5D, Table S18). For the highly abundant proteins in

DOI: 10.1021/acs.jproteome.7b00621
J. Proteome Res. XXXX, XXX, XXX−XXX

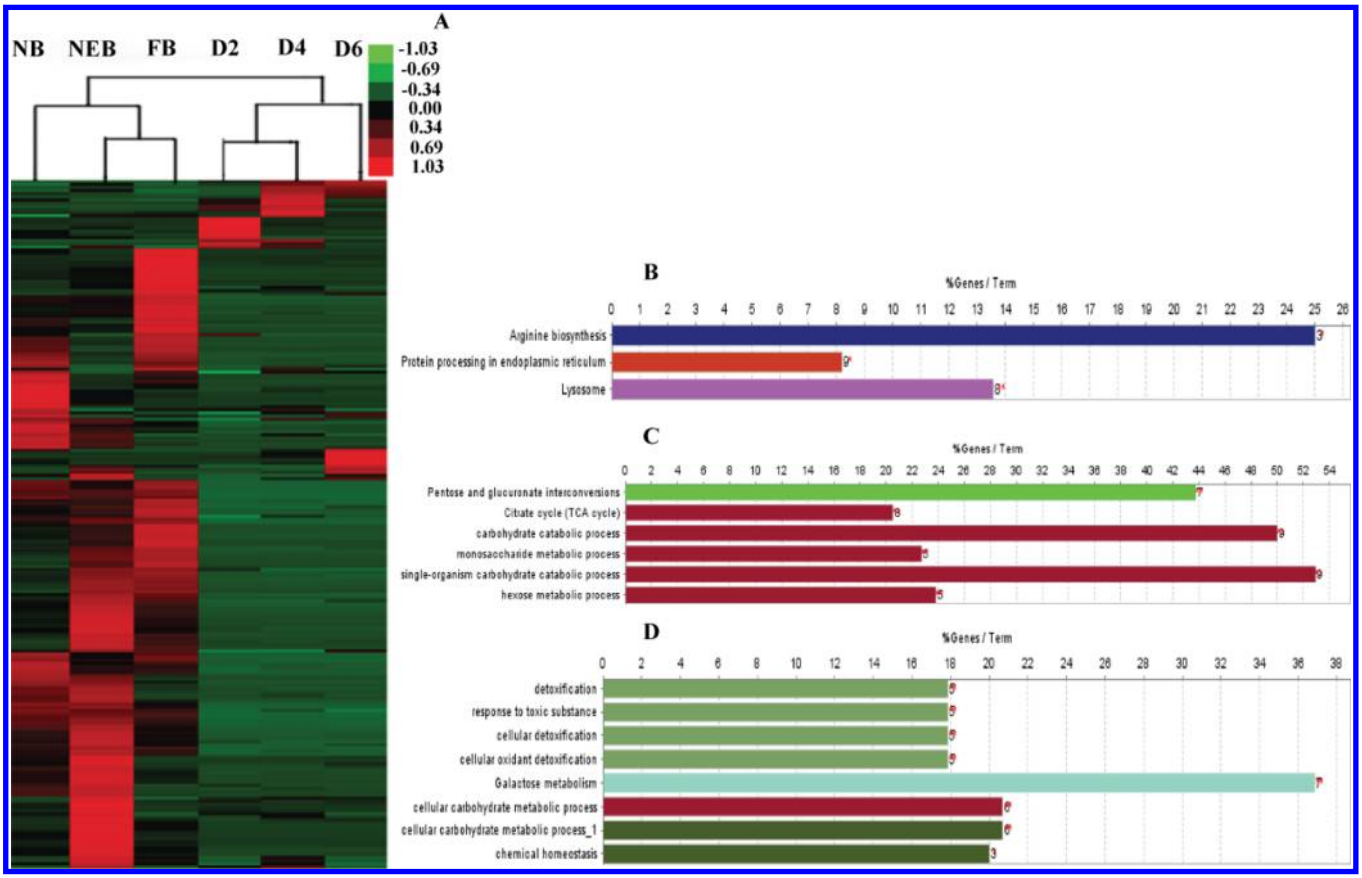

Figure 5. Quantitative comparison of ITb hemolymph proteins across six time points. The unsupervised hierarchical clustering analysis of proteins with altered abundance levels (fold change >1.5 and $p < 0.05$); the columns indicate the time points, and the rows represent individual proteins (A). The up-regulated proteins are indicated by red color and the down-regulated ones by green color. The color intensity changes with the protein expression level, as indicated on the key bar. Bar charts B, C, and D indicate uniquely enriched functional class and pathway in NEBs, NBs, and FBs, respectively. The single and double asterisks indicate significant enrichment at $p < 0.05$ and $p < 0.01$ statistical levels, respectively.

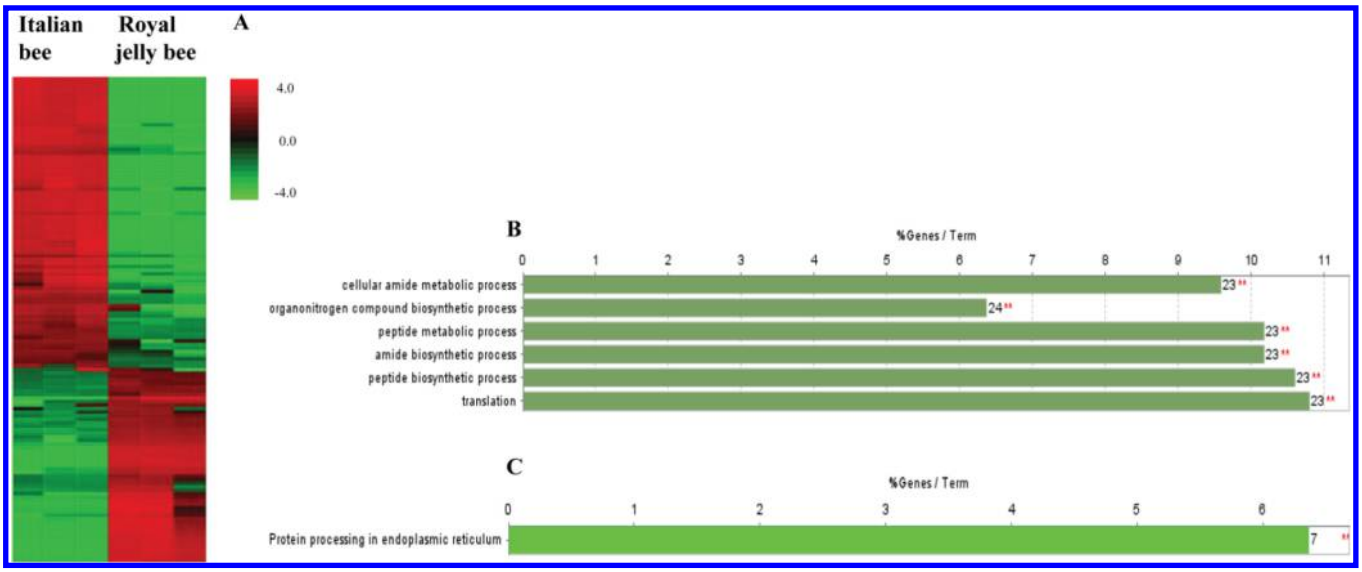

Figure 6. Quantitative comparison of hemolymph proteins between RJbs and ITbs in d2 larvae. The unsupervised hierarchical clustering analysis of proteins with altered abundance levels (fold change >1.5 and $p < 0.05$); the columns indicate the three replicates in each of the two bee strains, and the rows represent individual proteins (A). The up-regulated proteins are indicated by red color and the down-regulated ones by green color. The color intensity changes with the protein expression level, as shown on the key bar. Bar charts B and C represent enriched specific terms in the functional class and pathway in RJbs and ITbs, respectively. The single and double asterisks indicate significant enrichment at $p < 0.05$ and $p < 0.01$ statistical levels, respectively.

DOI: 10.1021/acs.jproteome.7b00621
J. Proteome Res. XXXX, XXX, XXX−XXX

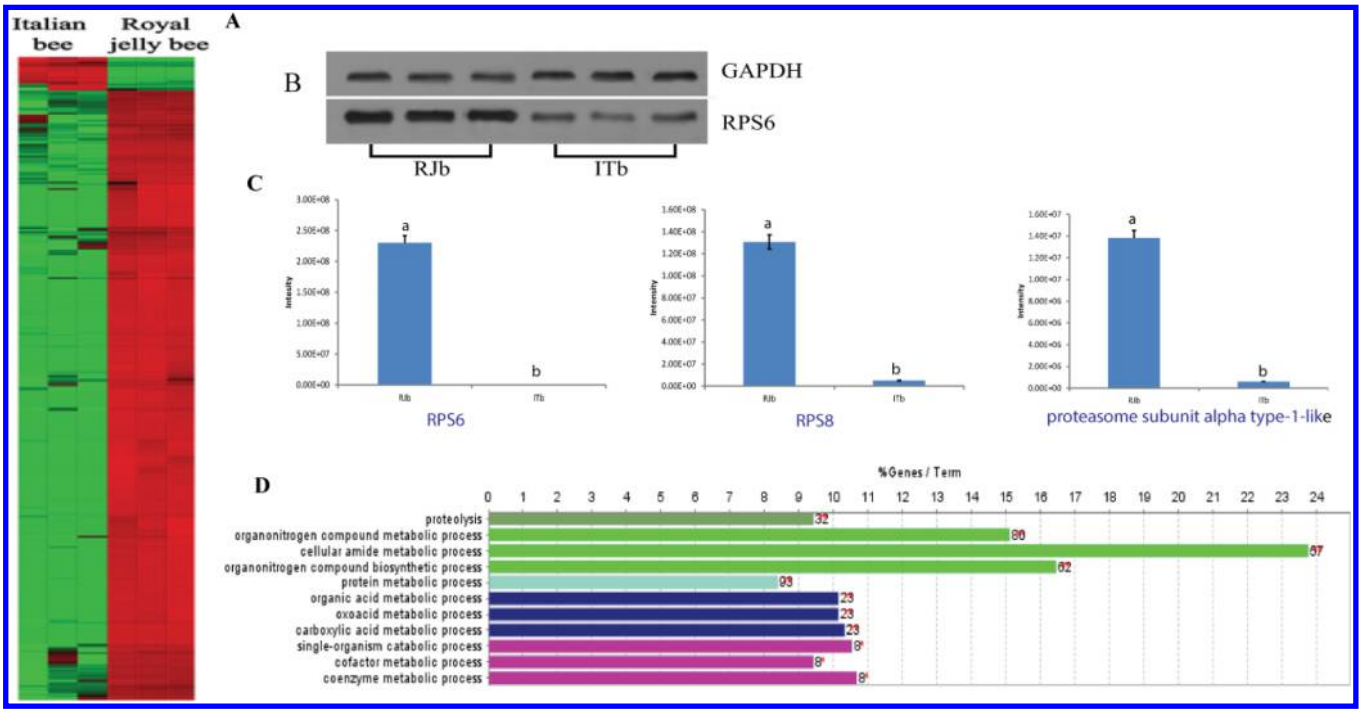

Figure 7. Quantitative comparison of hemolymph proteins between RJbs and ITbs in d4 larvae. The unsupervised hierarchical clustering analysis of proteins with altered abundance levels (fold change >1.5 and $p < 0.05$); the columns indicate the three replicates in each of the two bee strains, and the rows represent individual proteins (A). The up-regulated proteins are indicated by red color and the down-regulated ones by green color. The color intensity changes with the protein expression level as indicated on the key bar. B represents the Western blot of RpS6. C indicates representative protein expressional levels between RJbs and ITbs in d4 larvae, and "a" is significantly higher ($p < 0.05$) than "b". Bar chart D represents enriched specific terms in the functional classes and pathways in RJbs. The single and double asterisks indicate significant enrichment at $p < 0.05$ and $p < 0.01$ statistical levels, respectively.

the PPI network of ITbs in the adult ages, protein folding (q-value = 9.16×10^{-6}) and lipid oxidation (q-value = 7.01×10^{-3}) were significantly enriched in NEBs (Figure S2A); glycolysis (q-value = 1.14×10^{-4}) and single-organism carbohydrate metabolic process (q-value = 2.33×10^{-3}) were enriched in NBs (Figure S2B); and antioxidant activity (q-value = 2.07×10^{-8}), glycolysis (q-value = 5.15×10^{-4}), cellular homeostasis (q-value = 2.52×10^{-3}), and muscle contraction (q-value = 1.34×10^{-2}) were enriched in FBs (Figure S2C).

3.4. Hemolymph Proteome Comparison between RJbs and ITbs at Six Time Points

To better explore the differences in hemolymph proteome between the two bee strains, the proteomes of hemolymph at each time point of RJbs and ITbs were compared. In d2 larvae, of the 1130 proteins identified in hemolymph, 739 and 836 proteins were identified in RJbs and ITbs, respectively (Figure S3A, Tables S1 and S10). A functional class involved in translational elongation and pathways related to glycolysis/gluconeogenesis, proteasome, phagosome, lysosome, and arginine and proline metabolism were enriched in the two samples (Figure S3B, Table S19). Notably, pyridine nucleotide metabolic process, ribosome, and protein processing in ER were exclusively enriched in RJbs (Figure S3C, Table S19). In ITbs, ribose phosphate metabolic process, cysteine and methionine, and starch and sucrose were uniquely enriched (Figure S3D, Table S19). Among the differentially regulated 128 proteins, 49 and 79 were highly abundant in RJbs and ITbs, respectively (Figure 6A, Table S20). The 49 highly abundant proteins in RJbs were enriched in translational machinery (Figure 6B, Table S21). The highly abundant 79 proteins in ITbs were enriched in a pathway of protein processing in ER (Figure 6C, Table S21). Moreover, the highly abundant proteins in RJbs were significantly involved in ribosome in the PPI network (Figure S4A). Protein folding was enriched in the network of ITbs (Figure S4B).

In d4 larvae, 1322 and 1057 proteins were found in RJbs and ITbs, respectively, representing 1599 proteins (Figure S5A, Tables S2 and S11). Among the functional groups and pathways enriched, glycolysis/gluconeogenesis, pentose phosphate, and posttranscriptional regulation of gene expression were strongly enriched by both samples (Figure S5B, Table S22). Intriguingly, four functional categories, organonitrogen compound metabolic, small-molecule metabolic, carbohydrate derivative metabolic, and oxidation−reduction processes, and three pathways, purine metabolism, lysosome, and proteasome, were exclusively enriched in RJbs (Figure S5C, Table S22). However, only purine nucleoside triphosphate metabolic process was uniquely enriched in ITbs (Figure S5D, Table S22). Among the 1599 proteins in both strains, the expression levels of 358 proteins were altered, of which 341 were highly abundant in RJbs and 17 in ITbs (Figure 7A, Table S22). Notably, the 341 highly abundant proteins in RJbs were enriched in five functional groups and one pathway: cellular amide metabolic process, carboxylic acid metabolic process, cofactor metabolic process, protein metabolic process, and proteolysis (Figure 7B, Table S24). However, the 17 highly abundant proteins in ITbs were not significantly enriched in any functional group or pathway. Regarding the PPI network of RJbs, the highly abundant proteins were significantly enriched in ribosome, protein folding, and mRNA binding (Figure S6).

In d6 larvae, 813 and 820 proteins were identified in RJbs and ITbs, respectively, representing a total of 1130 proteins

DOI: 10.1021/acs.jproteome.7b00621
J. Proteome Res. XXXX, XXX, XXX−XXX

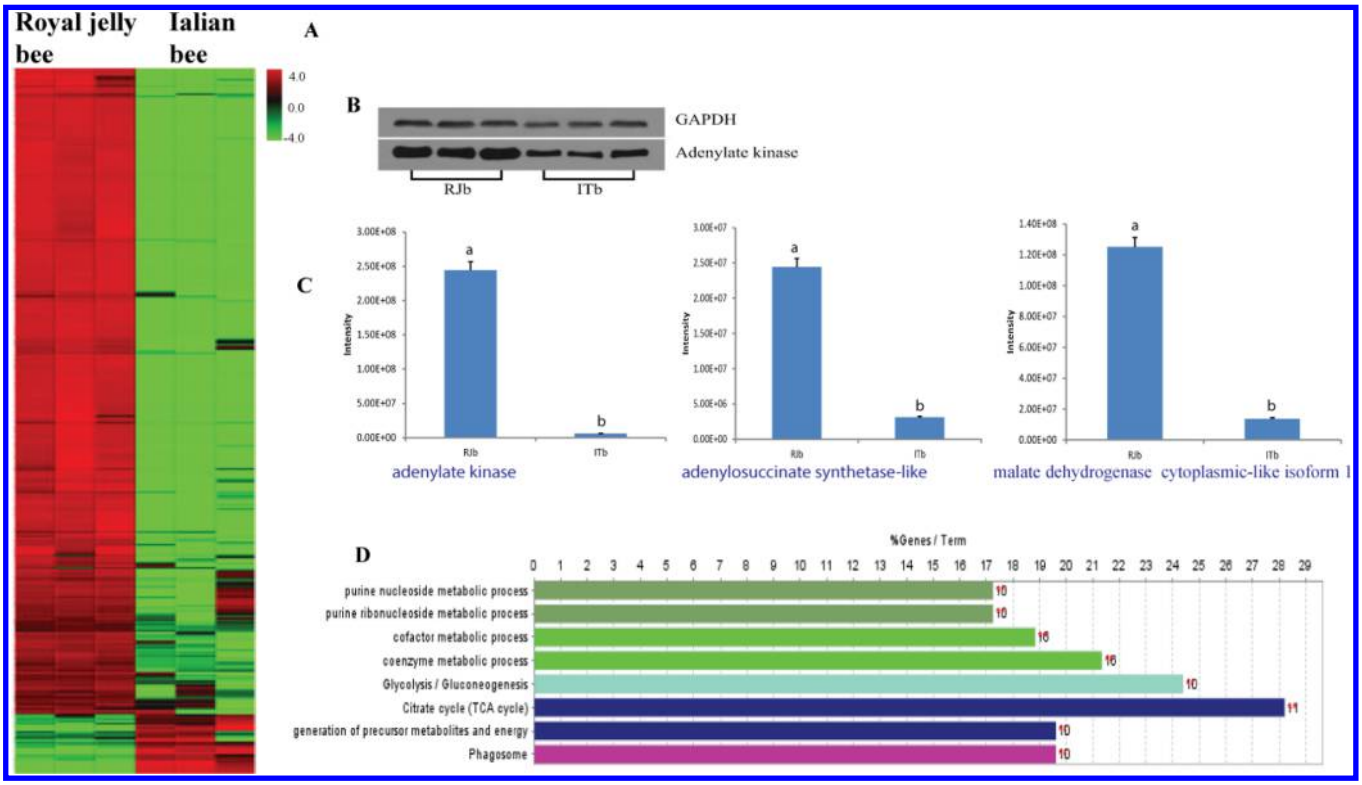

Figure 8. Quantitative comparison of hemolymph proteins between RJbs and ITbs in NBs. The unsupervised hierarchical clustering analysis of proteins with altered abundance levels (fold change >1.5 and $p < 0.05$); the columns indicate the three replicates in each of the two bee strains, and the rows represent individual proteins (A). The up-regulated proteins are indicated by red color and the down-regulated ones by green color. The color intensity changes with the protein expression level, as indicated on the key bar. B represents the Western blot of adenylate kinase. C indicates representative protein expressional levels between RJbs and ITbs in NBs and "a" is significantly higher ($p < 0.05$) than "b". Bar chart D represents enriched specific terms in the functional classes and pathways in RJbs. The one and two asterisks indicate significant enrichment at $p < 0.05$ and $p < 0.01$ statistical levels, respectively.

(Figure S7A, Tables S3 and S12). At this age, three functional classes and eight pathways were commonly enriched by the two samples. Organonitrogen compound metabolic process, pentose phosphate, and proteasome were among the strongly enriched functional groups and pathways (Figure S7B, Table S25). In RJbs, two functional classes, nucleoside diphosphate phosphorylation and purine-containing compound metabolic process, and two pathways, pentose and glucuronate interconversions and galactose metabolism, were uniquely enriched (Figure S7C, Table S25). In ITbs, carbohydrate metabolic and single-organism carbohydrate catabolic processes were significantly enriched (Figure S7D, Table S25). When evaluating the abundance level of 1130 proteins in both strains, 232 proteins were found to be regulated. Of these, 82 were highly abundant in RJbs and 150 in ITbs (Figure S8A, Table S26). The highly abundant proteins in RJbs were enriched in pyridine-containing compound metabolic process (Figure S8B, Table S27). The highly abundant proteins in ITbs were enriched in cellular homeostasis, aminoglycan metabolic process, pentose and glucuronate interconversions, amino sugar and nucleotide sugar metabolism, and pyruvate metabolism (Figure S8C, Table S27). Furthermore, proteins with high abundance level in RJbs were enriched in a positive regulation of melanin biosynthetic process and homeostatic process in the PPI network (Figure S9A). In ITbs, innate immune response was enriched in PPI network (Figure S9B).

In NEBs, of 1592 proteins, 1380 and 1014 were identified in RJbs and ITbs, respectively (Figure S10A, Tables S4 and S13). Two functional classes and seven pathways were commonly enriched in two samples. Sugar and nucleotide sugar metabolism, beta-alanine metabolism, fructose and mannose metabolism, and proteasome pathways were among the strongly enriched functional classes and pathways (Figure S10B, Table S28). In RJbs, five functional classes and five pathways, such as carboxylic acid process, small-molecule process, cellular homeostasis, phagosome, endocytosis, protein processing in ER, and galactose metabolism, were uniquely enriched (Figure S10C, Table S28). Only carbohydrate metabolic process was exclusively enriched in ITbs (Figure S10D, Table S28). When examining the abundance level of 1592 proteins in both strains, 173 proteins were found to be differentially regulated, of which 111 and 62 proteins were highly abundant in RJbs and ITbs, respectively (Figure S11A, Table S29). The proteins in high abundance levels in RJbs were enriched in four pathways: glyoxylate and dicarboxylate metabolism, fructose and mannose metabolism, cysteine and methionine metabolism, and glutathione metabolism (Figure S11B, Table S30). Again, the highly abundant proteins in ITbs were involved in two functional classes and two pathways, chitin metabolic process, dicarboxylic acid metabolic process, alanine, aspartate, and glutamate metabolism, and amino sugar and nucleotide sugar metabolism (Figure S11C, Table S30). In RJbs, proteins with altered abundance levels linked in the PPI network were involved in protein folding, generation of precursor metabolites and energy, and immune response (Figure S12A). In ITbs, the highly abundant proteins were implicated in antioxidant activity and generation of precursor metabolites and energy in the PPI network (Figure S12B).

DOI: 10.1021/acs.jproteome.7b00621
J. Proteome Res. XXXX, XXX, XXX−XXX

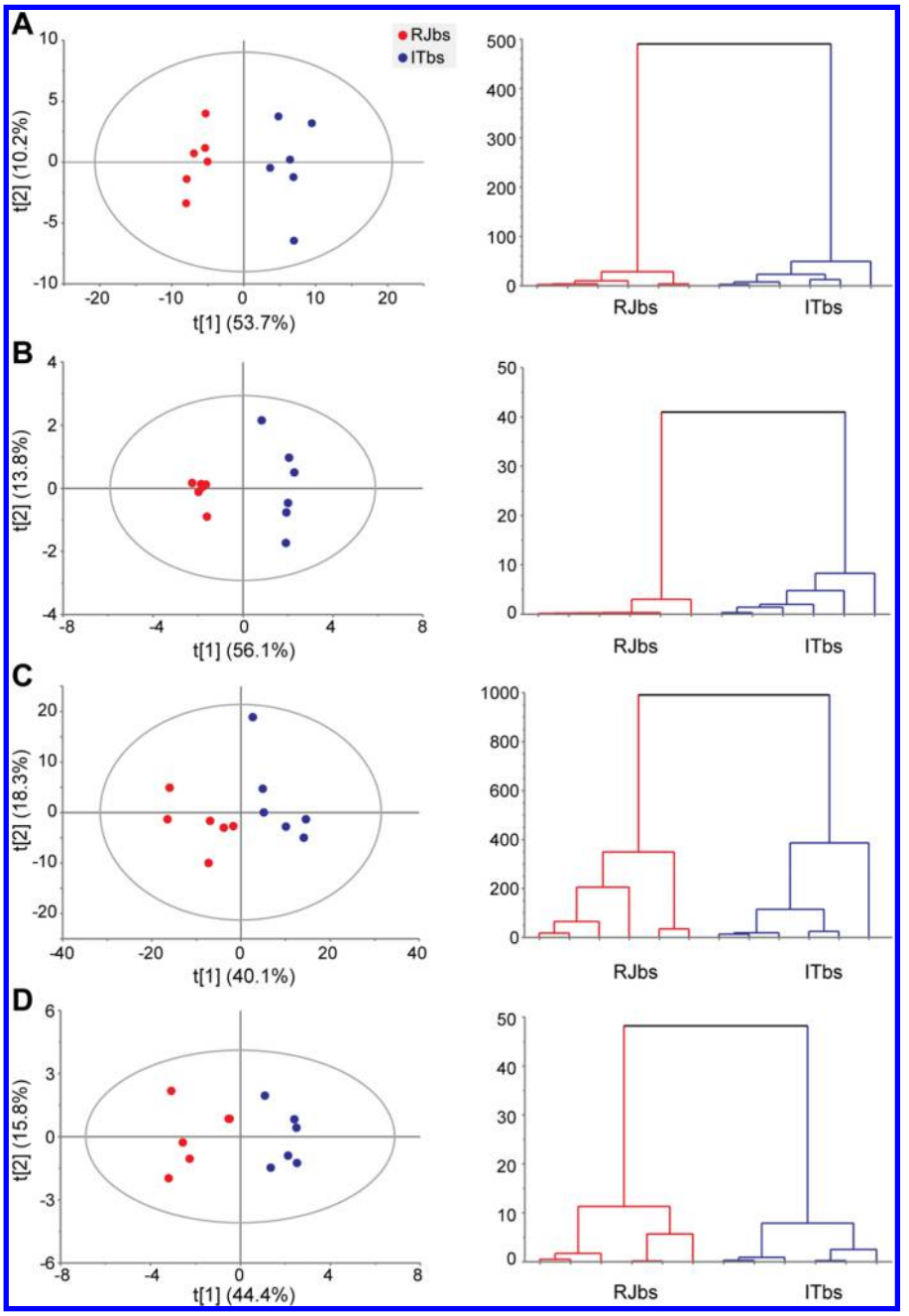

Figure 9. PCA score plots (left) and HCA dendrograms (right) for RJbs and ITbs. (A) d4 larvae in ESI+ mode; (B) d4 larvae in ESI− mode; (C) NBs in ESI+ mode; (D) NBs in ESI− mode. t[1] and t[2] represent the first and second principle components, respectively, with their values in parentheses. The PCA eclipse refers to the 95% confidence interval.

In NBs, 1457 and 1090 proteins were found in RJbs and ITbs, respectively (Figure S13A, Tables S5 and S14). They represented 2547 proteins, of which proteins involved in the generation of precursor metabolites and energy were enriched by both strains (Figure S13B, Table S31). Notably, in RJbs, four functional classes, carboxylic acid metabolic process, small-molecule metabolic process, cellular homeostasis, and oxidation−reduction, and four pathways, phagosome, protein processing in ER, amino sugar and nucleotide sugar metabolism, and galactose metabolism, were uniquely enriched (Figure S13C, Table S31). In ITbs, however, only pyridine nucleotide metabolic process was exclusively enriched (Figure S13D, Table S31). Among the 2547 proteins identified, 326 hemolymph proteins were found to be regulated in two samples. Of these, 297 and 29 proteins were highly abundant in RJbs and ITbs, respectively (Figure 8A, Table S32). Interestingly, in RJbs, the 297 highly abundant proteins were enriched in two functional classes and three pathways: coenzyme metabolic process, purine nucleoside metabolic process, citrate cycle (TCA cycle), glycolysis/gluconeogenesis, and phagosome (Figure 8B, Table S33), whereas in ITbs, the 29 highly abundant proteins were not enriched in any GO terms or pathways. Furthermore, in RJbs, the highly abundant proteins in the PPI network were enriched in antioxidant activity, generation of precursor metabolites and energy, protein folding, ion binding, and gland morphogenesis (Figure S14).

DOI: 10.1021/acs.jproteome.7b00621
J. Proteome Res. XXXX, XXX, XXX−XXX

In FBs, among 967 proteins, 710 and 759 were identified in RJbs and ITbs, respectively (Figure S15A, Tables S6 and S15). Two functional groups, purine nucleoside metabolic and single-organism carbohydrate metabolic processes, were enriched and shared by both strains (Figure S15B, Table S34). Remarkably, one functional class and one pathway, carbohydrate metabolic process and citrate cycle (TCA cycle), were uniquely enriched in RJbs (Figure S15C, Table S34), whereas no functional classes or pathways were enriched in ITbs. Of the 967 proteins in FBs, 77 proteins were significantly regulated, of which 31 and 46 were highly abundant in RJbs and ITbs, respectively (Figure S16A, Table S35). In RJbs, the highly abundant proteins were enriched in carbohydrate catabolic process (Figure S16B, Table S36). In ITbs, the highly abundant proteins were enriched in single-organism carbohydrate metabolic process (Figure S16C, Table S36). Regarding the regulated proteins in the PPI network of FBs, glycolysis and carbohydrate catabolic process were significantly enriched in RJbs (Figure S17A), and glycolysis was enriched in ITbs (Figure S17B).

3.5. Metabolome Comparison of Hemolymph between RJbs and ITbs at D4 Larvae and NBs

To validate the proteome differences between RJbs and ITbs at both d4 larvae and NB stage, a metabolomics analysis of their hemolymph was performed. Five injections of the QC sample were uniformly distributed in the analytical sequence to control system stability. The PCA score plots for all samples displayed a close clustering pattern of QCs for both ESI+ and ESI− modes (Figure S18), indicating the high stability and performance of the analytical platform. The clear separation between RJbs and ITbs at both ages in PCA score plots and HCA dendrograms (Figure 9) indicates the different metabolomics profiles between them. Among the differential features (VIP values >1 in OPLS-DA and p values <0.05 in the Student's t-test) that mainly contributed to the discrimination of d4 larvae between RJbs and ITbs, 24 and 29 compounds were identified in ESI+ and ESI− modes, respectively (Table S37). Among them, 10 differential compounds were commonly identified in both modes. A total of 20 and 29 compounds in NBs between RJbs and ITbs were identified in ESI+ and ESI− modes, respectively, and six of them were identified in both modes (Table S37). These differential compounds were enriched mainly in pathways involved in amino acid metabolism, protein synthesis (e.g., aminoacyl-tRNA biosynthesis), and energy metabolism (e.g., citrate cycle and oxidative phosphorylation) (Table S38).

4. DISCUSSION

We report a hitherto unexplored in-depth proteome coverage in the hemolymph of both bee stocks. This is a significant extension from previous proteins identified in hemolymph of the honeybees.[13,29,12] The expanded coverage of hemolymph proteome is mainly attributed to sampling at six time points over the larval and adult stages in two bee stocks as compared with using only one pupal sample.[29] The hemolymph in its entirety is found to perform biological functions that are molecularly distinct based on age in both bee stocks. In larvae, the change in proteome is supposed to support the larval development and immune defense.[9] In adults, the change in proteome is believed to modulate tissue development and immunity. Notably, RJbs have adapted hemolymph proteome settings quite divergent from ITbs to prime the differentiated physiology as a response to four decades of selection for increasing RJ yields.

4.1. Larvae Develop a Specific Hemolymph Proteome To Match with Age-Specific Physiology

During the 6 days of the larval stage, a 1500-fold increase in body weight occurs.[40] To establish this exponential growth, a common and age-specific hemolymph proteome is employed. This is reflected by the enriched multiple ranges of shared function classes related to protein synthesis, energy metabolism, immune responses, and cellular homeostasis in both bee lines across the larval stages. Protein synthesis is of fundamental importance for larval growth, organogenesis, and immune defense.[9] Energy metabolism is vital for fueling metabolic energy for the growth and organogenesis of the larvae.[13] The age-dependent hemolymph proteome settings reflected by uniquely enriched functional groups and pathways is therefore suggestive of their roles in underlining a specific physiology at each age. During the early age, larval growth depends on rapid cell division and thus requires amino acids for protein synthesis and nucleotide metabolism as nuclear material for cell division.[41] We show that beta-alanine metabolism is uniquely enriched in d2 larvae of both strains and nucleotide phosphorylation is enriched in d2 RJb larvae but not in d4 and d6 larvae. This indicates the importance of amino acid and nucleotide synthesis in initiating young larval growth. Nucleotide phosphorylation plays a key role in the synthesis of nucleotides that are required for a variety of cellular metabolic processes, such as RNA and DNA synthesis.[42] A stronger expression of ndk/awd involved in this functional class highlights the high need for synthesis of nucleotides for the young larvae. Moreover, ndk/awd is involved in the degradation pathway that delivers amino acids for the synthesis of new proteins during early pupal stage of the honeybee.[9,10] Because of its nonsubstrate specific nature as an enzyme for cellular metabolism, ndk/awd uses the ribose and deoxyribose forms of both purine and pyrimidine NDPs as a substrate. It is thus used for the synthesis of purine and pyrimidine bases,[43] which are essential nucleotide precursors for cell nuclei and differentiation of cells.[43] These findings suggest that the d2 larvae develop a high demand for amino acids and nucleotides to support their growth through rapid cell division, as is the case in young embryos.[24]

Larvae younger than 2 days lack innate immunity because their immunity has not yet been established.[3,44] In this context, the acquired immunity from ingredients of larval food (royalisin, major royal jelly proteins (MRJPs), etc.),[10,45] is pivotal to ensuring normal larval development. The highly nutritive MRJPs are key in both larval growth and immune defense of the honeybees.[3] In this study, we found that in d2 larvae the highly abundant MRJP1 and MRJP3 precursors in both bees signify their centrality in enhancing larval development and temporal immune defense. This is consistent with the high abundance of MRJP1 found in hemolymph of young larvae (<day 3) to boost their body development and immunity.[9] The presence of MRJP1 precursor represents the need for essential amino acids and its role in stimulating macrophages.[46] Moreover, MRJP3 precursor plays a role as a nitrogen reserve for larval growth[46] and for its potential immuno-regulatory property.[47] Furthermore, the uniquely enriched lysosome pathway in d2 ITb larvae, reflects its role in the immunity of young larvae. Lysosomes receive and degrade both complex molecules and pathogenic proteins[48] and are fused with the plasma membrane during cell injury,[49] suggesting the lysosome pathway's role in supporting the weak innate immunity of young larvae. For instance, V-type proton

DOI: 10.1021/acs.jproteome.7b00621
J. Proteome Res. XXXX, XXX, XXX−XXX

ATPase is required for lysosomal acidification and is thus essential for the activation of degradative enzymes located within the lysosomal lumen for the degradation of Notch and the export of degradation products via coupled transporters.[50] It also regulates Notch cleavage by providing a rationale for physiological and pathological endocytic control of Notch activity.[51] All in all, the immune-related proteins found in the hemolymph of d2 larvae are critical in supporting their weak immunity, whereas the enriched lysosomes support normal larval growth.[10]

The larvae of middle age (3 to 4 days) need the highest amounts of protein[52] to support the largest growth in larval development that begins around the fourth day.[53] In our study, the exclusively enriched oxidation−reduction, and alanine, aspartate, and glutamate metabolism in both strains and protein processing in ER, and endocytosis in d4 RJbs may serve the purpose. The protein processing in ER functions in proper folding, preparing for targeting and membrane attachment of newly translated proteins,[54] and endocytosis is key to transporting plasma membrane proteins into the cell interior.[55] The enriched protein processing in ER and endocytosis suggests that d4 larvae require newly synthesized proteins as building molecules for developing organs and constructing tissues[10] as well as for establishing immune defense.[48] For example, heat shock proteins (HSPs) in protein processing in ER are pivotal in protein quality control during and after protein biosynthesis,[9] and assist nascent protein folding during early larval development of the honeybee.[56] As a potent immunogen,[57] HSPs are also involved in the activation of immune defense against invasive pathogens.[9,58] Moreover, the uniquely enriched ribosome pathway by highly abundant proteins in d4 RJbs larvae reflects the vital activity of protein synthesis in driving rapid larval growth and tissue construction. Protein synthesis machinery and ribosomal proteins (Rps) in larval hemolymph are decreasing with increasing age of the larvae.[13] However, the higher number of up-regulated Rps (9) in d4 as compared with in d2 larvae (only 1 Rp) suggests the enhanced activity in protein synthesis to support rapid growth of larvae, which is inconsistent with the previous report.[13] For instance, the highly abundant RpL35 is vital in facilitating cell cycle in the first gap phase of interphase when a cell physically grows larger and makes the molecular building blocks.[59] Rpl23a is associated with protein synthesis, folding, and sorting[60] and may play a key role in the activation of the immune defense, which is the case in termites.[61] Furthermore, the highly abundant proteins enriched in translational elongation in the PPI network of RJbs larvae suggests that translational machinery is also critical for larval growth and immune defense. Overall, the d4 larvae are in a developmental stage that demands high protein molecules to support body growth[9] and build immunity.[29]

This fast larval growth also requires intensive molecular fuel for organ and tissue construction.[9,10] To this end, the enriched functional groups related to energy turnover, such as small-molecule metabolic process and galactose metabolism in d4 larvae of both strains, are thought to serve as fuel generators. Carbohydrate metabolism acts as a source of energy for the metamorphosis of growing larvae.[10] The stronger expression of pyruvate carboxylase mitochondrial isoform X1 in ITbs and ATP-citrate synthase isoformX1 in d4 of both stocks reflects their crucial roles in energy metabolism. Pyruvate carboxylase, which catalyzes the ATP-dependent carboxylation of pyruvate to oxaloacetate, is an important intermediate in gluconeogenesis and de novo fatty acid synthesis.[62] ATP-citrate synthase is critical for central energy metabolism of aerobic organisms, catalyzing the condensation of acetyl-CoA and oxaloacetate to form citrate.[63] Notably, the enriched GO terms and strongly expressed proteins in d4 larvae of both lines that are involved in energy production suggest that metabolic energy is key to driving the high-energy demand during organogenesis at this age.[9]

The d6 time point is the end of the larval phase, marked by the beginning of metamorphosis at which complex reorganization of larval structures occurs.[64] The uniquely enriched pyridine nucleotide metabolic process in d6 larvae of RJbs suggests its role in regulating energy metabolism for the beginning of organ reconstruction. Pyridine nucleotide is pivotal in serving as a coenzyme for various dehydrogenase enzymes to regulate cellular metabolism and the rate of ATP production.[65] Furthermore, the uniquely enriched lipid transport by highly abundant proteins in d6 RJbs is in agreement with the increase in transporter proteins with increasing larval age.[13] In insects, apolipophorin III (ApoLp-III)-like protein precursor is primarily expressed in body fat and released into the hemolymph as a lipid transporter during flight.[66] An increased abundance of ApoLp-III in the hemolymph with increasing larval age is important for larval development of the honeybee.[13] These observations suggest that at the end of the larval phase specific energy transport develops to fuel the complex reorganization of larval structures.

4.2. Adult Worker Bees Evolve Age-Dependent Hemolymph Proteome to Prime Age-Related Biology

Worker bees perform age-related tasks during adult life, which are often associated with changes in physiology correlated with age and differences in morphology.[67] The commonly enriched functions related to protein synthesis, energy metabolism, amino acid metabolism, and response to immune defense and toxic substances across the adult ages of both stocks are suggestive of their centrality in supporting biological demands. Age-dependent hemolymph function during adult ages, however, is reflected by the age-specifically enriched and activated functional classes and pathways. In NEBs, the glands are already formed once they emerge from the comb cells but not fully developed.[22] Hemolymph at this age contains low protein owing to extensive protein depletion during the nonfeeding period associated with body reconstruction.[11] Thus protein supplementation is required to prime growth and immune defense. To support this development, proteins have to be synthesized as tissue blocks to cement normal cell growth and tissue construction in NEBs.[22,30] The enriched peptide biosynthetic process in the NEBs of RJbs implies the importance of proteins to prime development and physiology of the glands. The increased rate of the elongation phase of protein synthesis is crucial for increasing total protein in adult *Drosophila*, which is correlated with fast polypeptide chain elongation in *Drosophila*.[68] This elongation of polypeptide chain is mediated by higher activity of elongation factors 1-alpha (EF1a) in the whole body of young *Drosophila*.[69] Hence, the strongly expressed proteins related to peptide biosynthesis in the NEBs indicate their vital roles in protein synthesis in stimulating growth of young bees, as it does in *Drosophila*.[68,69] The high abundance of folding proteins and the enhanced protein processing in ER of NEBs are suggestive of the fact that voluminous protein molecules are required to promote tissue development. The increased abundance level of proteins related

DOI: 10.1021/acs.jproteome.7b00621
J. Proteome Res. XXXX, XXX, XXX−XXX

to immunity of NEBs, such as HSPs and calreticulin, indicate their roles in the immune activation against pathogens and stress.[9,11] These findings are suggestive of the fact that protein synthesis is vital to stimulating growth of NEBs as well as preconditioning them to new stress upon leaving the closed environment of the capped comb.

The main task of NBs is to take care of the brood by feeding RJ secreted from the HGs.[70,71] To drive RJ synthesis and secretion, the NBs require a great amount of proteins and metabolic energy.[20] The uniquely enriched organonitrogen compound metabolic process in both strains, protein catabolic process, and RNA transport in NBs of RJbs are indicative of their roles in proteins synthesis to consolidate RJ secretion.[22] RNA transport plays a role in the coordination of important physiological processes, including regulation of development and allocation of nutrition,[72] which is also highlighted by the uniquely enriched RNA transport pathway in NBs. Moreover, the strongly expressed proteins enriched in RNA transport pathway in NBs of RJbs, relative to in NEBs and FBs, further underscore the significance of protein synthesis to prompt RJ secretion in the HGs. For instance, eIF-1a and eIF-5a assist the proper positioning of the small ribosomal subunit to start codon,[73] and the presence of eIF-4e is essential for cap binding and the subsequent RNA helicase activities leading to protein translation.[73] Synthesis and secretion of RJ by NBs also demands much metabolic energy.[22] The highly abundant proteins like pyruvate kinase-like isoform X1 and phosphoglycerate kinase isoform 1, involved in energy metabolism in NBs in both stocks, indicate the stronger energy requirement of NBs to attain the high secretory synthesis.[20]

For FBs, the main mission is to collect the food the colony needs from the wild.[40] The uniquely enriched pyridine-containing compound metabolic process in FBs of ITbs indicates the importance of energy during task shift. Pyridine nucleotide is one of the pyridine-containing compounds that regulates the rate of ATP synthesis by acting as electron carrier in mitochondria via the electron-transport chain and oxidative phosphorylation.[65] Furthermore, the enriched citrate metabolism in RJbs and cellular carbohydrate metabolism in ITbs by highly abundant proteins suggest that carbohydrate is the primary energy source used during foraging flights.[74] This also indicates that metabolic specialization that occurs during the social ontogeny of worker bees meets their metabolic energy demand and utilization.[75] This is in line with the fact that enzymes involved in sugar uptake and processing are in higher abundance in the HGs of FBs compared with those of NBs.[76] Moreover, high abundance of α-glucosidase found here in ITbs is in agreement with the elevated level of α-glucosidase found in the whole body sample of FBs,[75] suggesting the importance of carbohydrate as an energy source in FBs. This evidence supports the previous[75] finding that a higher capacity of carbohydrate energy processing is present in the hemolymph of FBs to fuel foraging flights.

4.3. RJbs and ITbs Adapt Divergent Hemolymph Proteome Programs During Larval to Adult Stages

To better understand the molecular basis that derives the differentiated physiology upon the selection for enhanced RJ yields in RJbs, the proteomes at each time point were compared between both stocks. In d2 larvae, RJbs and ITbs have developed distinct proteome programs by uniquely enriched functions in each strain such as nucleotide and protein synthesis in d2 RJbs larvae and metabolizing energy related pathways in ITbs. The enriched ribosome in d2 larvae of RJbs further supports its importance in driving organogenesis by providing protein molecules for fast growth[24] and its significance in boosting larval immunity.[3,28] Moreover, the highly abundant EF1a and many Rps involved in translational machinery in d2 larvae of RJbs, relative to ITbs, suggest that protein synthesis for organ and tissue formation may be enhanced.

At 3 to 4 days, the larvae begin the largest body growth[53] by increasing the frequency of food intake.[52] In this context, the commonly enriched functional terms related to metabolic energy production and protein synthesis in d4 larvae of both strains suggest the significance of protein and metabolic fuel, similar to the aforementioned larval growth. Notably, a higher number of uniquely enriched functional terms implicated in metabolizing energy, protein synthesis, and antioxidant activities in RJbs, as compared with only one related to metabolizing energy in ITbs, indicates profound proteome difference at this time point. To be noted, the enriched functional terms such as protein metabolism, proteolysis, and carboxylic acid metabolism by the highly abundant proteins (341) in RJbs, relative to in ITbs, is in sharp contrast with non-GO term enriched by the up-regulated proteins (17) in ITbs, relative to in RJbs. Protein metabolism is pivotal for the synthesis of new proteins to support large body growth of the larvae.[9] Proteolysis as cellular housekeeping pathways support larval growth by recycling misfolded proteins to make new proteins.[77] Furthermore, the highly abundant Rps unique to RJbs indicate their vital roles. RpS6 (validated by Western blot) and RpS8 (25-fold), for example, are involved in protein metabolism. Proteasome subunit alpha type-1-like (25-fold) and proteasome subunit beta type-2-like isoform 1 (unique to RJbs) are implicated in proteolysis and indicate their vital roles for larval development through protein synthesis, cell-cycle regulation, and immune responses.[78−80] Together with distinct metabolomics profiles, this indicates that the d4 larvae have evolved a distinct developmental trajectory between both bee stocks driven by protein synthesis and energy metabolism in response to selection pressure for higher RJ production.

The older aged larvae accumulate sufficient energy[3] to prepare for the upcoming energy depletion that occurs during reorganization of larval structures.[64] Here the commonly enriched functions related to energy metabolism in both stocks indicate the importance of metabolic energy for metamorphosis. However, the two stocks have evolved distinct energy turnover strategies to support the reorganization of larval structures during the later larval phase.[64] This is reflected in the exclusively enriched functions associated with energy metabolism such as pentose and glucuronate interconversions in RJbs and carbohydrate metabolism in ITbs. Moreover, the highly abundant proteins in RJbs enriched in pyridine-containing compound and those in ITbs enriched in four functional groups related to energy metabolism further suggest that energy plays key a role for this phase of larval growth.

In NEBs, the highly abundant proteins enriched in glyoxylate and in dicarboxylate and fructose and mannose metabolisms in RJbs and dicarboxylic acid metabolic process and alanine, aspartate, and glutamate in ITbs are indicative of the needs for energy to initiate the synthesis of new proteins.[11] However, the highly abundant proteins enriched in cysteine and methionine metabolism in RJbs, relative to in ITbs, are suggestive of the fact that NEBs of RJbs have a stronger demand of amino acids for protein synthesis to underline the growth of task-related glands.[81] Furthermore, the highly abundant proteins enriched

DOI: 10.1021/acs.jproteome.7b00621
J. Proteome Res. XXXX, XXX, XXX−XXX

in glutathione metabolism in RJbs relative to in ITbs signify their importance for cellular homeostasis. For instance, the induced enzymes in the glutathione S-transferase family imply preconditioning of NEBs to new stress upon leaving the capped comb[11] and possession of a pro-inflammatory function on immune response.[82] These findings manifest that genetic selection for the high RJ output has altered the proteome signatures of RJbs to adapt to a distinct cellular homeostasis during the transition from larval to adult phase.

The main biological duty of NBs is correlated with glandular development,[40] which demands numerous anatomical and physiological changes in preparation for brood nursing, including the growth of HGs and MGs.[30,83] To secrete RJ for larvae, NBs require proteins for the development of their glands.[20] Hence, proteins related to energy metabolism, protein synthesis, and cellular homeostasis are vital to underpin high RJ secretion via provision of biological molecules for RJ synthesis and cell maintenance.[22] The enriched wide array of GO terms involved in metabolizing energy, protein synthesis, and cellular homeostasis in RJbs, as compared with ITbs, suggests that RJb has reshaped its hemolymph proteome arsenals to respond to the selection of increased RJ yields. This is in line with the profound metabolomics difference that NBs at this age require high metabolic energy to facilitate proper cell divisions toward normal morphological and physiological development of HG.[20] This is likely due to the fact that NBs of RJbs have evolved stronger activity of HGs and a higher metabolism level to fit their elevated level of RJ secretion[84] compared with NBs of ITbs. Notably, of the differential proteins (326 proteins) in NBs between both lines (297 in RJbs and 29 in ITbs), the highly abundant proteins enriched in TCA cycle, coenzyme metabolic process, and glycolysis in NBs of RJbs, as compared with in NBs of ITbs, indicate that energy metabolism is enhanced to ensure fulfilment of the demand of the glandular system[67] for higher RJ secretion. A typical example is adenylate kinase (50 times higher in RJbs as validated by Western blot), a phosphotransferase enzyme involved in purine nucleoside metabolism, which is critical in energy homeostasis.[85] This is in agreement with the finding that RJb NBs have a stronger metabolic energy demand than ITbs to facilitate physiology of the glands in order to synthesize and secrete RJ in the HGs. This is also supported by the significantly higher RJ production in RJbs.

For FBs, intensive energy is demanded to fuel foraging activity (i.e., collecting food resources).[74] This is reflected by the commonly enriched functional terms related to energy metabolism in the FBs of both stocks. However, the uniquely enriched carbohydrate-related energy metabolism in FBs of RJbs, as compared with the nonfunctional term enriched by FBs of ITbs, indicates that FBs of RJbs require a relatively high amount of energy to support their foraging flight. Moreover, the highly abundant proteins in RJbs involved in carbohydrate catabolism further suggest a high demand for carbohydrate energy to fuel-foraging flight.[74] This can possibly be explained by the fact that FBs of RJbs have developed a stronger tendency to collect pollen,[23] which, in turn, increases the pollen supply for RJb NBs to stimulate their elevated RJ secretion.[83]

5. CONCLUSIONS

Our unprecedented in-depth proteome coverage in the hemolymph of honeybees reveals that the hemolymph proteome in both bee lines underlines age-dependent biology. During the larval stage, the proteome may drive development and immune defense. The d2 larvae need a temporal immune protection mechanism to support the immature immune system and larval growth. The d4 larvae demand intensive energy and protein biosynthesis to underpin rapid organogenesis and immune defense, and energy transport is necessary to fuel the complex reorganization of larval structures in d6 larvae. In adults, the functionally enhanced protein synthesis, energy metabolism, and antioxidants may boost tissue development and immunity in NEBs, gland physiology in NBs, and energy turnover in FBs. Furthermore, the two bee stocks adapt distinct proteome architectures to prime the differentiated physiology owing to decades of selection for high RJ production in RJbs. Notably, the RJbs have evolved a quite divergent hemolymph proteome arsenals, particularly in day 4 larvae and NBs, to consolidate a physiology that supports higher RJ secretion by providing protein biomolecules and metabolic energy. Our data provide novel insight into molecular details that drive both hemolymph function and high RJ production of RJbs.

■ ASSOCIATED CONTENT

Supporting Information

The Supporting Information is available free of charge on the ACS Publications website at DOI: 10.1021/acs.jproteome.7b00621.

Figure S1. PPI network of the highly abundant proteins expressed across six time points of RJbs. Figure S2. PPI network of the highly abundant proteins expressed over six time points of ITbs. Figure S3. Qualitative comparison of hemolymph proteins between RJbs and ITbs in d2 larvae. Figure S4. PPI network of the highly abundant proteins expressed in d2 larvae between RJbs and ITbs. Figure S5. Qualitative comparison of hemolymph proteins between RJbs and ITbs in d4 larvae. Figure S6. PPI network of the highly abundant proteins expressed in d4 larvae between RJbs and ITbs. Figure S7. Qualitative comparison of hemolymph proteins between RJbs and ITbs in d6 larvae. Figure S8. Quantitative comparison of hemolymph proteins between RJbs and ITbs in d6 larvae. Figure S9. PPI network of the highly abundant proteins expressed in d6 larvae between RJbs and ITbs. Figure S10. Qualitative comparison of hemolymph proteins between RJbs and ITbs in NEBs. Figure S11. Quantitative comparison of hemolymph proteins between RJbs and ITbs in NEBs. Figure S12. PPI network of the highly abundant proteins expressed in NEBs between RJbs and ITbs. Figure S13. Qualitative comparison of hemolymph proteins between RJbs and ITbs in NBs. Figure S14. PPI network of the highly abundant proteins expressed in NBs between RJbs and ITbs. Figure S15. Qualitative comparison of hemolymph proteins between RJbs and ITbs in FBs. Figure S16. Quantitative comparison of hemolymph proteins between RJbs and ITbs in FBs. Figure S17. PPI network of the highly abundant proteins expressed in FBs between RJbs and ITbs. Figure S18. PCA score plots of all hemolymph samples including QCs (in red) in ESI + and ESI− modes. (PDF)

Table S1: Identification of expressed hemolymph proteins of RJb worker in d2 larvae. Table S2: Identification of expressed hemolymph proteins of RJb worker in d4 larvae. Table S3: Identification of expressed

DOI: 10.1021/acs.jproteome.7b00621
J. Proteome Res. XXXX, XXX, XXX−XXX

hemolymph proteins of RJb worker in d6 larvae. Table S4: Identification of expressed hemolymph proteins of RJb worker in NEBs. Table S5: Identification of expressed hemolymph proteins of RJb worker in NBs. Table S6: Identification of expressed hemolymph proteins of RJb worker in FBs. Table S7: Biological process and pathway enrichment of the identified hemolymph proteins of RJb worker over the six time points. Table S8: Differentially expressed proteins in the hemolymph of RJbs over six time points. Table S9: Biological process and pathway enrichment of highly abundant proteins in the hemolymph of RJbs over six time points. Table S10: Identification of expressed hemolymph proteins of ITb worker in d2 larvae. Table S11: Identification of expressed hemolymph proteins of ITb worker in d4 larvae. Table S12: Identification of expressed hemolymph proteins of ITb worker in d6 larvae. Table S13: Identification of expressed hemolymph proteins of ITb worker in NEBs. Table S14: Identification of expressed hemolymph proteins of ITb worker in NBs. Table S15: Identification of expressed hemolymph proteins of ITb worker in FBs. Table S16: Biological process and pathway enrichment of the identified hemolymph proteins of ITb worker across six time points. Table S17: Differentially expressed proteins in the hemolymph of ITbs over six time points. Table S18: Biological process and pathway enrichment of highly abundant proteins in the hemolymph of ITbs over six time points. Table S19: Comparison of biological process and pathway enrichment of the hemolymph proteins identified in d2 larvae of RJbs and ITbs. Table S20: Differentially expressed proteins in the hemolymph between RJbs and ITbs in d2 larvae. Table S21: Comparison of functional GO term enrichment of proteins highly abundant in the hemolymph of RJbs and ITbs in d2 larvae. Table S22: Comparison of biological process and pathway enrichment of the hemolymph proteins identified in RJbs and ITbs in d4 larvae. Table S23: Differentially expressed proteins in the hemolymph between RJbs and ITbs in d4 larvae. Table S24: Comparison of functional GO term enrichment of proteins highly abundant in the hemolymph of RJbs and ITbs in d4 larvae. Table S25: Comparison of biological process and pathway enrichment of the hemolymph proteins identified in RJbs and ITbs in d6 larvae. Table S26: Differentially expressed proteins in the hemolymph between RJbs and ITbs in d6 larvae. Table S27: Comparison of functional GO term enrichment of proteins highly abundant in the hemolymph of RJbs and ITbs in d6 larvae. Table S28: Comparison of biological process and pathway enrichment of the hemolymph proteins identified in RJbs and ITbs in NEBs. Table S29: Differentially expressed proteins in the hemolymph between RJbs and ITbs in NEBs. Table S30: Comparison of functional GO term enrichment of proteins highly abundant in the hemolymph of RJbs or ITbs in NEBs. Table S31: Comparison of biological process and pathway enrichment of the hemolymph proteins identified in RJbs and ITbs in NBs. Table S32: Differentially expressed proteins in the hemolymph between RJbs and ITbs in NBs. Table S33: Comparison of functional GO term enrichment of proteins highly abundant in the hemolymph of RJbs in NBs. Table S34: Comparison of biological process and pathway enrichment of the hemolymph proteins identified in RJbs and ITbs in FBs. Table S35: Differentially expressed proteins in the hemolymph between RJbs and ITbs in FBs. Table S36: Comparison of functional GO term enrichment of highly abundant proteins in the hemolymph of RJbs or ITbs in FBs. Table S37. Differential compounds identified in d4 larvae between RJbs and ITbs in ESI+ and ESI− modes. Table S38. Pathway analysis of the differential compounds identified in d4 larvae and NBs between RJbs and ITbs. (XLSX)

AUTHOR INFORMATION

Corresponding Author

*Tel/Fax: +86 10 8210 6448. E-mail: apislijk@126.com.

ORCID

Bin Han: 0000-0001-6974-8699

Jianke Li: 0000-0003-4183-7336

Author Contributions

†Z.A. and C.M. contributed equally to this work.

Notes

The authors declare no competing financial interest.

ACKNOWLEDGMENTS

This work is supported by the Agricultural Science and Technology Innovation Program (CAAS-ASTIP-2015-IAR) and the earmarked fund for Modern Agro-Industry Technology Research System (CARS-44) in China.

REFERENCES

(1) Vierstraete, E.; Cerstiaens, A.; Baggerman, G.; Van Den Bergh, G.; De Loof, A.; Schoofs, L. Proteomics in Drosophila melanogaster: First 2D database of larval hemolymph proteins. *Biochem. Biophys. Res. Commun.* **2003**, *304*, 831−838.

(2) Chan, Q. W. T.; Howes, C. G.; Foster, L. J. Quantitative comparison of caste differences in honeybee hemolymph. *Mol. Cell. Proteomics* **2006**, *5* (12), 2252−2262.

(3) Chan, Q. W.; Melathopoulos, A. P.; Pernal, S. F.; Foster, L. J. The innate immune and systemic response in honey bees to a bacterial pathogen, Paenibacillus larvae. *BMC Genomics* **2009**, *10*, 387.

(4) Kim, T.; Kim, Y.-J. Overview of innate immunity in. *Drosophila. J. Biochem. Mol. Biol.* **2005**, *38* (2), 121−127.

(5) Strand, M. R. The insect cellular immune response. *Insect Sci.* **2008**, *15*, 1−14.

(6) Randolt, K.; Gimple, O.; Geissendörfer, J.; Reinders, J.; Prusko, C.; Mueller, M. J.; Albert, S.; Tautz, J.; Beier, H. Immune-related proteins induced in the hemolymph after aseptic and septic injury differ in honey bee worker larvae and adults. *Arch. Insect Biochem. Physiol.* **2008**, *69*, 155−167.

(7) Flatt, T.; Heyland, A.; Rus, F.; Porpiglia, E.; Sherlock, C.; Yamamoto, R.; Garbuzov, A.; Palli, S. R.; Tatar, M.; Silverman, N. Hormonal Regulation of the Humoral Innate Immune Response in. *J. Exp. Biol.* **2008**, *211* (16), 2712−2724.

(8) Erban, T.; Jedelsky, P. L.; Titera, D. Two-dimensional proteomic analysis of honeybee, *Apis mellifera*, winter worker hemolymph. *Apidologie* **2013**, *44*, 404−418.

(9) Feng, M.; Ramadan, H.; Han, B.; Fang, Y.; Li, J. Hemolymph proteome changes during worker brood development match the biological divergences between western honey bees (Apis mellifera) and eastern honey bees (Apis cerana). *BMC Genomics* **2014**, *15*, 563.

(10) Woltedji, D.; Fang, Y.; Han, B.; Feng, M.; Li, R.; Lu, X.; Li, J. Proteome analysis of hemolymph changes during the larval to pupal

DOI: 10.1021/acs.jproteome.7b00621
J. Proteome Res. XXXX, XXX, XXX−XXX

development stages of honeybee workers (*Apis mellifera ligustica*). *J. Proteome Res.* **2013**, *12*, 5189−5198.
(11) Erban, T.; Harant, K.; Kamler, M.; Markovic, M.; Titera, D. Detailed proteome mapping of newly emerged honeybee worker hemolymph and comparison with the red-eye pupal stage. *Apidologie* **2016**, *47*, 805−817.
(12) Erban, T.; Petrova, D.; Harant, K.; Jedelsky, P. L.; Titera, D. Two-dimensional gel proteome analysis of honeybee, *Apis mellifera*, worker red-eye pupa hemolymph. *Apidologie* **2014**, *45*, 53−72.
(13) Chan, Q. W. T.; Foster, L. J. Changes in protein expression during honey bee larval development. *Genome Biol.* **2008**, *9*, R156. .1−14.
(14) Gatschenberger, H.; Gimple, O.; Tautz, J.; Beier, H. Honey bee drones maintain humoral immune competence throughout all life stages in the absence of vitellogenin production. *J. Exp. Biol.* **2012**, *215*, 1313−1322.
(15) Chen, S.; Su, S.; Lin, X. An introduction to high-yielding royal jelly production methods in China. *Bee World* **2002**, *83* (2), 69−77.
(16) Cao, L.-F.; Zheng, H.-Q.; Pirk, C. W. W.; Hu, F.-L.; Xu, Z.-W. High Royal Jelly-Producing Honeybees (*Apis mellifera ligustica*) (Hymenoptera: Apidae) in China. *J. Econ. Entomol.* **2016**, *109*, 510.
(17) Li, J.-K.; Chen, S.-L.; Zhong, B.-X.; Su, S. Genetic analysis for developmental behavior of honeybee colony's royal jelly production traits in western honeybees. *Acta Genet. Sin.* **2003**, *30* (6), 547−554.
(18) Zhang, L.; Li, J. ke; Wu, L. ming. Profile Analysis of the Proteome of the Egg of the High Royal Jelly Producing Bees (*Apis mellifera* L.). *Agric. Sci. China* **2007**, *6* (9), 1138−1148.
(19) Chen, S.-L.; Li, J.; Zhong, B.-X.; Su, S.-K. Microsatellite analysis of royal jelly producing traits of Italian honeybee (*Apis mellifera liguatica*). *Acta Genet. Sin.* **2005**, *32* (10), 1037−1044.
(20) Jianke, L.; Mao, F.; Begna, D.; Yu, F.; Aijuan, Z. Proteome comparison of hypopharyngeal gland development between Italian and royal jelly producing worker honeybees (*Apis mellifera* L.). *J. Proteome Res.* **2010**, *9*, 6578−6594.
(21) Li, J.; Feng, M.; Zhang, Z.; Pan, Y. Identification of the proteome complement of hypopharyngeal glands from two strains of honeybees (*Apis mellifera*). *Apidologie* **2008**, *39*, 199−214.
(22) Feng, M.; Fang, Y.; Li, J. Proteomic analysis of honeybee worker (*Apis mellifera*) hypopharyngeal gland development. *BMC Genomics* **2009**, *10*, 645.
(23) Han, B.; Fang, Y.; Feng, M.; Hu, H.; Qi, Y.; Huo, X.; Meng, L.; Wu, B.; Li, J. Quantitative Neuropeptidome Analysis Reveals Neuropeptides Are Correlated with Social Behavior Regulation of the Honeybee Workers. *J. Proteome Res.* **2015**, *14*, 4382−4393.
(24) Fang, Y.; Feng, M.; Han, B.; Lu, X.; Ramadan, H.; Li, J. In-depth Proteomics Characterization of Embryogenesis of the Honey Bee Worker (*Apis mellifera ligustica*). *Mol. Cell. Proteomics* **2014**, *13* (9), 2306−2320.
(25) Fang, Y.; Feng, M.; Han, B.; Qi, Y.; Hu, H.; Fan, P.; Huo, X.; Meng, L.; Li, J. Proteome analysis unravels mechanism underling the embryogenesis of the honeybee drone and its divergence with the worker (*Apis mellifera lingustica*). *J. Proteome Res.* **2015**, *14*, 4059−4071.
(26) Qi, Y.; Fan, P.; Hao, Y.; Han, B.; Fang, Y.; Feng, M.; Cui, Z.; Li, J. Phosphoproteomic Analysis of Protein Phosphorylation Networks in the Hypopharyngeal Gland of Honeybee Workers (*Apis mellifera ligustica*). *J. Proteome Res.* **2015**, *14*, 4647−4661.
(27) Hernandez, L. G.; Lu, B.; Da Cruz, G. C. N.; Calabria, L. K.; Martins, N. F.; Togawa, R.; Espindola, F. S.; Yates, J. R.; Cunha, R. B.; De Sousa, M. V. Worker honeybee brain proteome. *J. Proteome Res.* **2012**, *11* (3), 1485−1493.
(28) Han, B.; Zhang, L.; Feng, M.; Fang, Y.; Li, J. An integrated proteomics reveals pathological mechanism of honeybee (*Apis cerena*) sacbrood disease. *J. Proteome Res.* **2013**, *12*, 1881−1897.
(29) Hu, H.; Bienefeld, K.; Wegener, J.; Zautke, F.; Hao, Y.; Feng, M.; Han, B.; Fang, Y.; Wubie, A. J.; Li, J. Proteome analysis of the hemolymph, mushroom body, and antenna provides novel insight into honeybee resistance against varroa infestation. *J. Proteome Res.* **2016**, *15*, 2841−2854.
(30) Huo, X.; Wu, B.; Feng, M.; Han, B.; Fang, Y.; Hao, Y.; Meng, L.; Wubie, A. J.; Fan, P.; Hu, H.; et al. Proteomic Analysis Reveals the Molecular Underpinnings of Mandibular Gland Development and Lipid Metabolism in Two Lines of Honeybees (*Apis mellifera ligustica*). *J. Proteome Res.* **2016**, *15*, 3342−3357.
(31) Zhang, J.; Xin, L.; Shan, B.; Chen, W.; Xie, M.; Yuen, D.; Zhang, W.; Zhang, Z.; Lajoie, G. a.; Ma, B. PEAKS DB: De Novo Sequencing Assisted Database Search for Sensitive and Accurate Peptide Identification. *Mol. Cell. Proteomics* **2012**, *11* (4), M111.010587.
(32) Lin, H.; He, L.; Ma, B. A combinatorial approach to the peptide feature matching problem for label-free quantification. *Bioinformatics* **2013**, *29* (14), 1768−1775.
(33) Bindea, G.; Mlecnik, B.; Hackl, H.; Charoentong, P.; Tosolini, M.; Kirilovsky, A.; Fridman, W.; Pagès, F.; Trajanoski, Z.; Galon, J.; et al. ClueGO : a Cytoscape plug-in to decipher functionally grouped gene ontology and pathway annotation networks. *Bioinformatics* **2009**, *25* (8), 1091−1093.
(34) Warde-Farley, D.; Donaldson, S. L.; Comes, O.; Zuberi, K.; Badrawi, R.; Chao, P.; Franz, M.; Grouios, C.; Kazi, F.; Lopes, C. T.; et al. The GeneMANIA prediction server: Biological network integration for gene prioritization and predicting gene function. *Nucleic Acids Res.* **2010**, *38*, W214−220.
(35) Tautenhahn, R.; Patti, G. J.; Rinehart, D.; Siuzdak, G. XCMS Online: a web-based platform to process untargeted metabolomic data. *Anal. Chem.* **2012**, *84* (11), 5035−5039.
(36) Kessner, D.; Chambers, M.; Burke, R.; Agus, D.; Mallick, P. ProteoWizard: Open source software for rapid proteomics tools development. *Bioinformatics* **2008**, *24* (21), 2534−2536.
(37) Dunn, W. B.; Broadhurst, D.; Begley, P.; Zelena, E.; Francis-McIntyre, S.; Anderson, N.; Brown, M.; Knowles, J. D.; Halsall, A.; Haselden, J. N.; et al. Procedures for large-scale metabolic profiling of serum and plasma using gas chromatography and liquid chromatography coupled to mass spectrometry. *Nat. Protoc.* **2011**, *6* (7), 1060−1083.
(38) López-Ibáñez, J.; Pazos, F.; Chagoyen, M. MBROLE 2.0-functional enrichment of chemical compounds. *Nucleic Acids Res.* **2016**, *44* (W1), W201−W204.
(39) Benjamini, Y.; Hochberg, Y. Controlling the False Discovery Rate : A Practical and Powerful Approach to Multiple Testing. *J. R. Stat. Soc., Ser. B (Methodol.)* **1995**, *57* (1), 289−300.
(40) Winston, M. L. *The Biology of the Honey Bee*; Harvard University Press: Cambridge, U.K., 1987; pp 46−71.
(41) PRICE, G. M. Protein and nucleic acid metabolism in insect fat body. *Biol. Rev.* **1973**, *48*, 333−372.
(42) Van Rompay, A. R.; Johansson, M.; Karlsson, A. Phosphorylation of nucleosides and nucleoside analogs by mammalian nucleoside monophosphate kinases. *Pharmacol. Ther.* **2000**, *87*, 189−198.
(43) Chakrabarty, A. M. Nucleoside diphosphate kinase: Role in bacterial growth, virulence, cell signalling and polysaccharide synthesis. *Mol. Microbiol.* **1998**, *28* (5), 875−882.
(44) Brodsgaard, C. J.; Ritter, W.; Hansen, H. Response of in vitro reared honey bee larvae to various doses of *Paenibacillus larvae* larvae spores. *Apidologie* **1998**, *29*, 569−578.
(45) Bilikova, K.; Wu, G. S.; Simuth, J. Isolation of a peptide fraction from honeybee royal jelly as a potential antifoulbrood factor. *Apidologie* **2001**, *32*, 275−283.
(46) Fratini, F.; Cilia, G.; Mancini, S.; Felicioli, A. Royal Jelly: An ancient remedy with remarkable antibacterial properties. *Microbiol. Res.* **2016**, *192*, 130−141.
(47) Li, J.; Wang, T.; Zhang, Z.; Pan, Y. Proteomic analysis of royal jelly from three strains of western honeybees (*Apis mellifera*). *J. Agric. Food Chem.* **2007**, *55*, 8411−8422.
(48) Sardiello, M.; Palmieri, M.; di Ronza, A.; Medina, D. L.; Valenza, M.; Gennarino, V. A.; Di Malta, C.; Donaudy, F.; Embrione, V.; Polishchuk, R. S.; et al. A Gene Network Regulating Lysosomal Biogenesis and Function. *Science* **2009**, 473−477.
(49) Luzio, J. P.; Pryor, P. R.; Bright, N. A. Lysosomes: fusion and function. *Nat. Rev. Mol. Cell Biol.* **2007**, *8*, 622−632.

DOI: 10.1021/acs.jproteome.7b00621
J. Proteome Res. XXXX, XXX, XXX−XXX

(50) Toei, M.; Saum, R.; Forgac, M. Regulation and isoform function of the V-ATPases. *Biochemistry* **2010**, *49*, 4715−4723.
(51) Vaccari, T.; Duchi, S.; Cortese, K.; Tacchetti, C.; Bilder, D.; et al. The vacuolar ATPase is required for physiological as well as pathological activation of the Notch receptor. *Development* **2010**, *137*, 1825−1832.
(52) Brouwers, E. V. M.; Ebert, R.; Beetsma, J. Behavioral and physiological aspects of nurse bees in relation to the composition of larval food during caste differentiation in the honeybee. *J. Apic. Res.* **1987**, *26* (1), 11−23.
(53) Bishop, G. H.; Briggs, A. P.; Ronzoni, E. Chemistry of Bee Larval Blood. *J. Biol. Chem.* **1925**, *66*, 77−88.
(54) Wünschiers, R. Posttranslational Modification of Proteins. In *Biochemical Pathways: An Atlas of Biochemistry and Molecular Biology*; Michal, G., Schomburg, D., Eds.; John Wiley & Sons, Inc.: Hoboken, NJ, 2012; pp 238−243.
(55) Just, W. Transport through Membranes. In *Biochemical Pathways: An Atlas of Biochemistry and Molecular Biology*; Michal, G., Schomburg, D., Eds.; John Wiley & Sons, Inc.: Hoboken, NJ, 2012; pp 272−278.
(56) Li, J.; Wu, J.; Rundassa, D. B.; Song, F.; Zheng, A.; Fang, Y. Differential protein expression in honeybee (*Apis mellifera* L.) larvae: Underlying caste differentiation. *PLoS One* **2010**, *5* (10), e13455.
(57) Ranford, J.; Coates, A.; Henderson, B. Chaperonins are Cell-Signa Signaling Proteins: The Unfolding Biology of Mollecular Chaperones. *Expert Rev. Mol. Med.* **2000**, *2*, 1−17.
(58) Guedes, S. D. M.; Vitorino, R.; Tomer, K.; Domingues, M. R. M.; Correia, A. J. F.; Amado, F.; Domingues, P. *Drosophila melanogaster* larval hemolymph protein mapping. *Biochem. Biophys. Res. Commun.* **2003**, *312*, 545−554.
(59) Babiano, R.; de la cruz, J. Ribosomal protein l35 is required for 27sb pre-rrna processing in *Saccharomyces cerevisiae*. *Nucleic Acids Res.* **2010**, *38* (15), 5177−5192.
(60) Hu, P.; He, X.; Zhu, C.; Guan, W.; Ma, Y. Cloning and characterization of a ribosomal protein L23a gene from Small Tail Han sheep by screening of a cDNA expression library. *Meta Gene* **2014**, *2*, 479−488.
(61) Liu, L.; Li, G.; Sun, P.; Lei, C.; Huang, Q. Experimental verification and molecular basis of active immunization against fungal pathogens in termites. *Sci. Rep.* **2015**, *5*, 15106.
(62) Jitrapakdee, S.; Nezic, M. G.; Cassady, A. I.; Khew-Goodall, Y.; Wallace, J. C. Molecular cloning and domain structure of chicken pyruvate carboxylase. *Biochem. Biophys. Res. Commun.* **2002**, *295*, 387−393.
(63) Wiegand, G.; Remington, S. J. CITRATE SYNTHASE: Structure, Control, and Mechanism. *Annu. Rev. Biophys. Biophys. Chem.* **1986**, *15*, 97−117.
(64) Gätschenberger, H.; Azzami, K.; Tautz, J.; Beier, H. Antibacterial Immune Competence of Honey Bees (*Apis mellifera*) Is Adapted to Different Life Stages and Environmental Risks. *PLoS One* **2013**, *8* (6), e66415.
(65) Nakamura, M.; Bhatnagar, A.; Sadoshima, J. Overview of Pyridine Nucleotides Review Series. *Circ. Res.* **2012**, *111*, 604−611.
(66) Weers, P. M. M.; Ryan, R. O. Apolipophorin III: Role model apolipoprotein. *Insect Biochem. Mol. Biol.* **2006**, *36*, 231−240.
(67) Crane, E. *Bees and Beekeeping: Science, Practice & World Resources*; Heinemann Newnes: Oxford, U.K., 1990; pp 62−64.
(68) Webster, G. C. Protein Synthesis. In *Drosophila as a Model Organism for Ageing Studies*; Lints, F. A., Soliman, M. H., Eds.; Blackie and Son Ltd.: London, 1988; pp 119−128.
(69) Webster, G. C.; Webster, S. L. Decline in synthesis of elongatiion factor oone (EF-I) precedes the decreased synthesis of total protein in aging Drosophila melanogaster. *Mech. Ageing Dev.* **1983**, *22*, 121−128.
(70) Ohashi, K.; Sasaki, M.; Sasagawa, H.; Nakamura, J.; Natori, S.; Kubo, T. Functional flexibility of the honey bee hypopharyngeal gland in a dequeened colony. *Zool. Sci.* **2000**, *17* (8), 1089−1094.
(71) Schneider, S. S. The Honey Bee Colony: Life History. In *The Hive and the Honey Bee*; Graham, J. M., Ed.; Dadant & Sons, Inc., Hamilton, IL, 2015; pp 73−109.
(72) Kehr, J.; Buhtz, A. Long distance transport and movement of RNA through the phloem. *J. Exp. Bot.* **2007**, *59* (1), 85−92.
(73) Hernández, G.; Vazquez-Pianzola, P. Functional diversity of the eukaryotic translation initiation factors belonging to eIF4 families. *Mech. Dev.* **2005**, *122*, 865−876.
(74) Suarez, R. K.; Darveau, C. A.; Welch, K. C., Jr.; O'Brien, D. M.; Roubik, D. W.; Hochachka, P. W. Energy metabolism in orchid bee flight muscle: carbohydrate fuels all. *J. Exp. Biol.* **2005**, *208*, 3573−3579.
(75) Wolschin, F.; Amdam, G. V. Comparative proteomics reveal characteristics of life-history transitions in a social insect. *Proteome Sci.* **2007**, *5*, 10.
(76) Ohashi, K.; Natori, S.; Kubo, T. Change in the mode of gene expression of the hypopharyngeal gland cells with an age-dependent role change of the worker honeybee *Apis mellifera* L. *Eur. J. Biochem.* **1997**, *249*, 797−802.
(77) Vierstra, R. D. Proteolysis in plants: mechanisms and functions. *Plant Mol. Biol.* **1996**, *32*, 275−302.
(78) Goh, S.-H.; Hong, S.-H.; Hong, S.-H.; Lee, B.-C.; Ju, M.-H.; Jeong, J.-S.; Cho, Y.-R.; Kim, I.-H.; Lee, Y.-S. eIF3m expression influences the regulation of tumorigenesis-related genes in human colon cancer. *Oncogene* **2011**, *30*, 398−409.
(79) Sun, C.; Todorovic, A.; Querol-audí, J.; Bai, Y.; Villa, N.; Snyder, M.; Ashchyan, J.; Lewis, C. S.; Hartland, A.; et al. Functional reconstitution of human eukaryotic translation initiation factor 3 (eIF3). *Proc. Natl. Acad. Sci. U. S. A.* **2011**, *108* (51), 20473−20478.
(80) Tsvetkov, P.; Mendillo, M. L.; Zhao, J.; Carette, J. E.; Merrill, P. H.; Cikes, D.; Varadarajan, M.; van Diemen, F. R.; Penninger, J. M.; Goldberg, A. L.; et al. Compromising the 19S proteasome complex protects cells from reduced flux through the proteasome. *eLife* **2015**, *4*, e08467.
(81) Proud, C. G. Control of the translational machinery by amino acids. *Am. J. Clin. Nutr.* **2014**, *99*, 231S.
(82) Flanagan, J. U.; Smythe, M. L. Sigma-class glutathione transferases. *Drug Metab. Rev.* **2011**, *43* (2), 194−214.
(83) Corby-Harris, V.; Meador, C. A. D.; Snyder, L. A.; Schwan, M. R.; Maes, P.; Jones, B. M.; Walton, A.; Anderson, K. E. Transcriptional, translational, and physiological signatures of undernourished honey bees (*Apis mellifera*) suggest a role for hormonal factors in hypopharyngeal gland degradation. *J. Insect Physiol.* **2016**, *85*, 65−75.
(84) He, X. J.; Tian, L. Q.; Barron, A. B.; Guan, C.; Liu, H.; Wu, X. B.; Zeng, Z. J. Behavior and molecular physiology of nurses of worker and queen larvae in honey bees (*Apis mellifera*). *J. Asia-Pac. Entomol.* **2014**, *17*, 911−916.
(85) Fry, D. C.; Kuby, S. A.; Mildvan, A. S. ATP-binding site of adenylate kinase: mechanistic implications of its homology with ras-encoded p21, F1-ATPase, and other nucleotide-binding proteins. *Proc. Natl. Acad. Sci. U. S. A.* **1986**, *83*, 907−911.

DOI: 10.1021/acs.jproteome.7b00621
J. Proteome Res. XXXX, XXX, XXX−XXX